Open-culture biotechnological process for triacylglycerides and polyhydroxyalkanoates recovery from industrial waste fish oil under saline conditions

Lucía Argiz, Rebeca González-Cabaleiro, David Correa-Galeote, Ángeles Val del Río, Anuska Mosquera-Corral

Accepted Manuscript

How to cite:
Separation and Purification Technology, April 2021, 118805
https://doi.org/10.1016/j.seppur.2021.118805

Open-culture biotechnological process for triacylglycerides and polyhydroxyalkanoates recovery from industrial waste fish oil under saline conditions

Lucía Argiz [a] *, Rebeca González-Cabaleiro [b], David Correa-Galeote [c], Ángeles Val del Río [a], Anuska Mosquera-Corral [a]

[a] CRETUS Institute, Department of Chemical Engineering, Universidade de Santiago de Compostela, 15782 Santiago de Compostela, Galicia, Spain.

[b] Department of Biotechnology, Delft University of Technology, Van der Maasweg 9, 2629 HZ Delft, the Netherlands.

[c] Department of Microbiology and Institute of Water Research, Universidad de Granada, Granada, Spain.

* Corresponding author: luciaargiz.montes@usc.es

ABSTRACT

Industrial waste fish oil streams contain high concentrations of medium and long-chain fatty acids suitable to produce value-added compounds. However, to process them dilution is required, and the water produced in the fish-canning industry commonly contains high salinity, which might limit its reuse as a dilution stream. Although NaCl is well-known to negatively affect biological activity, its effect on triacylglycerides (TAG) and polyhydroxyalkanoates (PHA) storage has not been well studied yet. Here, it was explored if intracellular TAG and PHA production can be efficient under saline conditions (10 g NaCl/L). For that purpose, waste fish oil was valorised using a mixed microbial culture (MMC) in a two-stage process (culture selection plus accumulation). Results showed that salinity influenced not only the activity but the structure of the microbial communities developed in the bioreactors. The bacterial genera *Acinetobacter* and *Rhizobium* and the mold *Candida glaebosa* clade were observed as the storing microorganisms which abundance increased under saline conditions whereas *Dipodascus* and *Mortierella* notably decreased. Nonetheless, despite the osmotic stress, promising results were obtained and maximum intracellular accumulations of 54.2 wt % (TAG:PHA = 28:72, 0.131 $Cmmol_{TAG}/Cmmol_S$, 0.303 $Cmmol_{PHA}/Cmmol_S$) and 50.9 wt % (TAG:PHA = 63:37, 0.291 $Cmmol_{TAG}/Cmmol_S$, 0.114 $Cmmol_{PHA}/Cmmol_S$) were observed when PHA and TAG were preferentially stored, respectively.

Keywords: lipids; mixed microbial culture; polyhydroxyalkanoates; salinity; triacylglycerides.

1. INTRODUCTION

The fish-canning industry is characterized by the generation of large volumes of liquid effluents containing high concentrations of organic compounds including, in many cases, hydrophobic lipids [1]. When the canneries have their wastewater treatment, comprising an aerobic biological step, these organic compounds usually reduce the efficiency of this treatment by limiting oxygen transfer [2]. For this reason, these lipid-rich compounds are mostly removed and rejected before full stream treatment in the wastewater treatment plant [2,3].

Recently, waste fish oil has started to be considered as a sustainable and low-cost source for the obtainment of storage compounds as triacylglycerides (TAGs) [4] and polyhydroxyalkanoates (PHAs) [5,6], value-added precursors for the production of biofuels and biomaterials alternative to fossil-based products [1].

Tamis et al. [4] have shown the feasibility of recovering lipids as TAGs when directly feeding soybean oil to a mixed microbial culture (MMC) in a process consisting of two steps: enrichment of the microbial culture in microorganisms with a high storage ability, and maximization of the storage compounds accumulation.

Regarding PHA, its production from oily streams traditionally requires an additional pre-treatment unit for the obtainment of soluble compounds suitable for their bioconversion into PHAs (usually volatile fatty acids, VFAs) [7,8]. Nonetheless, Argiz et al. (2021) recently demonstrated the possibility of performing in the same enrichment unit, the transformation of a lipid-rich waste stream produced in the fish-canning industry into long-chain fatty acids (LCFAs) and glycerol. Given that these compounds are precursors of both TAGs and PHAs, Argiz et al. (2021) tried to identify those selective pressures that might control the selection of the dominant metabolic pathways. It was observed that uncoupling carbon and nitrogen feedings and limiting nitrogen availability in the medium

allowed to maximise PHA accumulation. On the contrary, when this feeding strategy was combined with low pH in the famine phase, TAG storage was promoted [9].

The enrichment of MMCs in populations with high storage capacity is commonly carried in sequencing batch reactors (SBR) operated under the feast/famine (F/F) regime. In these reactors, half of their volume is exchanged with the feeding stream at the end of the operational cycle. Consequently, when using extremely high-loaded oily streams as a substrate (chemical oxygen demand (COD) concentration between 2,000 – 2,500 g/L), large volumes of water are required for dilution, severely reducing process sustainability. To enhance resource efficiency the possibility of reusing a water stream produced in the same industry for dilution could be considered. For this purpose, the fact that, in many cases, the effluents generated in the fish-processing sector contain relatively high salt concentrations needs to be considered.

The negative effect of salt concentrations above 5 – 8 g NaCl/L over the microbial activity has been reported for conventional biological treatment systems [3], but the influence of salt over the accumulation of TAGs [10–13] and PHAs [14,15] was mainly studied concerning the use of pure cultures and easily metabolizable carbon sources. These studies indicate that, in general, external stress caused by salinity promoted the intracellular accumulation of both compounds although different sensitivities were observed mainly depending on the strain used. Regarding the effect of salinity over TAGs storage in MMCs there is no available information and concerning PHAs accumulation, only [16,17] tested its influence when using non-acclimated and acclimated open cultures, respectively. [16] considered concentrations up to 20 g NaCl/L and observed that maximum intracellular PHA storage decreased with the increase of NaCl in the medium. [17] demonstrated that the acclimation of the culture to salinity in the enrichment process

allowed for the obtention of a higher PHA production under saline conditions although concentrations over 5 g NaCl/L caused a decrease of the process productivity.

The objective of the present study is to evaluate if identified selective pressures (C and N feeding regime and pH, [9]) that allowed for preferential PHAs or TAGs storage from waste oil in a two-stage system would also work under saline conditions (10 g NaCl/L). This research is focused on the analysis of the effect of NaCl over the operational parameters controlling the process, the culture enrichment and its microbial diversity, the maximum storage capacity, and the process productivity. Therefore, this study provides valuable information regarding the feasibility of reusing saline effluents as dilution water in the waste oil valorisation process for TAG and PHA production.

2. MATERIALS AND METHODS

2.1 Experimental set-up

To evaluate the effect of salinity over the industrial waste fish oil valorisation process, two lab-scale bioreactors were operated: an enrichment unit (SBR-S) and an accumulation fed-batch reactor (FBR-S). This two-stage system was analogous to the described by [9], used as "control" (without salt) for comparative purposes. This consisted of an enrichment reactor (SBR-C) in which storing microorganisms were selected from activated sludge in the absence of salinity, and an accumulation reactor (FBR-C) inoculated with the biomass enriched in SBR-C.

2.1.1 Operation of the enrichment reactor (SBR-S)

The enrichment reactor (SBR-S) was inoculated with activated sludge from a full-scale reactor in operation at an industrial wastewater treatment plant treating fish-canning saline effluents (10 – 15 g NaCl/L). The SBR-S, with a working volume of 4 L, was

operated under the F/F regime in cycles as described in Figure SI 1. At the end of each cycle of 12 hours, half of the volume of the reactor (2 L) was exchanged, resulting in hydraulic and solid retention times of 24 hours. The SBR-S was continuously aerated and completely mixed with air flowing through two air diffusers located at the bottom. The temperature was controlled at 30 ± 3 ºC by a thermostatic bath (Techne Inc, USA), and the dissolved oxygen (DO) concentration was measured online using a portable multimeter (model HQ40d, Hach-Lange, USA). No pH controller was used.

The carbon source consisted of the oily fraction of a fish-canning industry effluent (waste fish oil) from canned tuna production (2 mL/cycle, equivalent to 114.5 Cmmol/cycle) (Table SI 1a), the same used in SBR-C [9]. To simulate its dilution with the effluent of the same factory, 10 g NaCl/L were added to a synthetic water stream (2 L/cycle) with the same composition as the one used in SBR-C (Table SI 1b).

2.1.2 Fed-batch accumulation experiments

The maximum intracellular (TAG and PHA) accumulation capacity of the culture was determined by the performance of accumulation fed-batch assays in a 4-L FBR-S inoculated with biomass from SBR-S obtained after the two last enrichment cycles previous to FBR-S start-up. Except for the feeding regime, which consisted of pulses (between 6 – 10) of 0.8 mL of oil (equivalent to 45.8 Cmmol/pulse) without nitrogen addition, the operational conditions were kept identical to those of the SBR-S (the salinity was maintained at 10 g NaCl/L). The microbial activity in the accumulation assays was monitored by the continuous measurement of DO concentration. A new substrate pulse was added once the DO concentration experienced an increment indicating that the waste fish oil from the previous pulse was consumed. Maximum accumulation capacity was assumed to be reached when DO concentrations remained close to saturation values after the addition of a pulse.

2.2 Operational periods

The SBR-S was operated for 122 days, subdivided into three operational periods (Table SI 2) defined by two nitrogen feeding strategies (period I vs. periods II and III) and two concentrations of sodium bicarbonate buffer ($NaHCO_3$) in the water stream used for dilution (periods I and II vs. period III). In each period, one enrichment cycle (days 22, 85, and 106) and one accumulation assay (days 29, 85, and 106) were characterized (Table SI 2). For comparative purposes, it was considered analogous operational periods from the systems operated under saline (SBR-S) and non-saline conditions (SBR-C) (I, II, III vs C-I, C-II, C-III, respectively).

Until day 62 (period I), C and N sources were fed simultaneously and in excess at the beginning of the cycle imposing a conventional aerobic dynamic feeding regime (ADF). In periods II and III (days 63 – 122), C and N feedings were uncoupled imposing the double growth limitation (DGL) strategy. C was still fed in excess at the beginning of the cycle but N was added limited at the end of the feast to assure its absence during this phase, and avoid the growth of non-storing populations. Until day 85 (period II), the amount of $NaHCO_3$ added in the nutrients solution was the same as in period I. From day 86 onwards (period III), its concentration was reduced (from 1.0 to 0.8 g $NaHCO_3$ added per cycle).

The operational cycles with ADF feeding (period I) and uncoupled DGL (periods II and III) are described in Figure SI 1.

2.3 Analytical methods and calculations

The pH value was measured with a pH and Ion-Meter (GLP 22 Crison, Spain) and the electrical conductivity with a conductivity meter (probe Sension + EC5 HACH, Spain). Total and volatile suspended solids (TSS and VSS) were measured according to

158 APHA/AWWA/WEF, (2017). The COD was determined according to [18]. Total COD
159 was measured in the raw sample ($_t$COD) whereas the soluble fraction ($_s$COD) and the
160 other analyses determined in the liquid fraction were performed in the centrifuged
161 (Centrifuge 5430 Eppendorf, USA) and filtered sample (0.45 μm pore size, cellulose-
162 ester membrane, Advantec, Japan). VFA were determined by gas chromatography (6850
163 Series II Agilent Technologies, USA), ions (Li^+, Na^+, K^+, Mg^{+2}, Ca^{+2}, Cl^-, NO_2^-, Br^-, NO_3^-
164 , PO_4^{-3}, SO_4^{-2}) by ion chromatography (861 Advanced Compact IC Metrohm,
165 Switzerland), and total organic carbon, inorganic carbon and total nitrogen (TOC, IC, and
166 TN, respectively) by catalytic combustion (TOC-L analyzer with the TNM- module,
167 TOC-5000 Shimadzu, Japan).

168 The content of biomass on intracellular TAGs and PHAs compounds was determined in
169 the lyophilized biomass samples according to [19]. Commercial calibration standards of
170 TAGs (palmitic-, stearic-, oleic-, and linoleic- acids) and PHAs (copolymer containing
171 88 % hydroxybutyrate (HB) and 12 % hydroxyvalerate (HV)) were used (Sigma Aldrich,
172 USA). The storage compounds content of the biomass samples was calculated on a mass
173 basis and expressed in dry weight (wt %) as a percentage of the measured VSS.

174 The elemental composition of the active biomass (X) was assumed to be $CH_{1.8}O_{0.5}N_{0.2}$
175 [9] and its mass was determined as the difference between the mass of VSS (total
176 biomass) and that of accumulated compounds (TAGs + PHAs). Regarding kinetic
177 parameters, specific maximum consumption ($-q_N$) and production (q_{TAG}, q_{PHA}, q_X) rates
178 were estimated from the maximum slopes of the curves describing the evolution of the
179 different parameters. q values were expressed as Cmmol/(Cmmol$_X$·h) except for q_X,
180 which was referred to the substrate (S) and defined as Cmmol/(Cmmol$_S$·h). Overall
181 production rates (Q), Cmmol/(L·h), were determined by multiplying q_{TAG} and q_{PHA} by
182 the active biomass concentration in the system (Cmmol$_X$/L). Production yields (Y),

183 expressed as Cmmol/Cmmol$_S$, were calculated by dividing the production rates by the
184 carbon source consumption rates.

185 **2.4. Microbial analysis**

186 Samples (33 – 175 mL) from the accumulation reactors FBR-S (with salt, this study) and
187 FBR-C (without salt, [9]) were used to perform a microbial diversity analysis. These
188 samples were centrifuged (14,000 rpm, 1 min), supernatants were discarded, and the
189 resulting biomass samples were frozen and kept at -20 °C. Total deoxyribonucleic acid
190 (DNA) content was extracted using the FastDNA SPIN Kit and the FastPrep 24-
191 Instrument (MP Biomedicals, Germany) according to the manufacturer's protocol. DNA
192 extracts were subjected to Illumina for bacterial 16S rRNA and fungal 18S rRNA
193 sequencing. Amplification was performed using the primers Pro341F and Pro805R [20]
194 and FungiQuantF and FungiQuantR [21] for *Bacteria* and *Fungi*, respectively. Default
195 settings were used for quality control, primer trimming, filtering, pre-clustering, and
196 chimera detection through Mothur V1.44.3. Operational taxonomic units (OTUs) were
197 assigned at the 97 % cut-off level. Singleton OTUs were removed for later analysis.
198 Finally, taxonomic classification was made by the 16S and 18S ribosomal database from
199 the National Center for Biotechnology Information (U.S.) using the blast tool of the
200 Geneious Prime v.2019 software (Geneious, U.S.). The 16S rRNA and 18S rRNA
201 sequences retrieved in this research work were deposited in GeneBank under the
202 accession numbers PRJNA701464.

203 To evaluate the effect of salinity over the bacterial and fungal communities, two
204 hierarchical clustering analyses were made considering the relative abundances (RAs) of
205 the main bacterial and fungal OTUs (RA > 0.5 %) found in each sample. Non-parametric
206 tests (Mann-Whitney and Kruskal Wallis) were used to analyse differences among
207 samples ($p < 0.05$).

208 ## 3. RESULTS AND DISCUSSION

209 ### 3.1 Waste fish oil valorisation under saline conditions

210 The medium salinity (10 g NaCl/L) did not affect the hydrolysis, and subsequent
211 metabolization of the waste fish oil fed to the enrichment reactor. Thus, the typical F/F
212 pattern in the SBR-S became apparent after only four days from the beginning of the
213 operation (eight enrichment cycles). DO concentration decreased after substrate feeding
214 and it was maintained at low values during carbon source consumption (feast phase).
215 Then it increased because of external substrate exhaustion (famine phase).

216 However, the culture accumulation capacity was found to be limited. Thus, the feast/cycle
217 length ratio obtained in period I was 0.31 ± 0.01, over the value of 0.25 found as optimum
218 [22]. This observation was confirmed by the complete characterization of an SBR-S
219 enrichment cycle carried after reaching stable operational performance (day 22) (Figure
220 1a) together with an accumulation batch assay in the FBR-S (day 29) (Figure 1d).
221 According to the kinetic parameters and production yields observed during the feast phase
222 (Table 1a), the high values obtained concerning q_X, q_N and Y_X suggest that high N
223 availability in the medium promoted extracellular carbon source consumption for growth
224 instead of its intracellular storage. With a TAG:PHA ratio of 96:4, the culture was able
225 to accumulate about 17 wt % at the end of the feast phase and maximum intracellular
226 storage in the FBR-S was even lower (13.5 wt %).

227 At this point, the need for process optimization to increase maximum storage capacity
228 and productivity was clear. With this objective, those selective pressures favouring
229 preferential TAG or PHA production when using a non-pre-fermented hydrophobic
230 substrate identified in [9], were tested here under saline conditions.

231

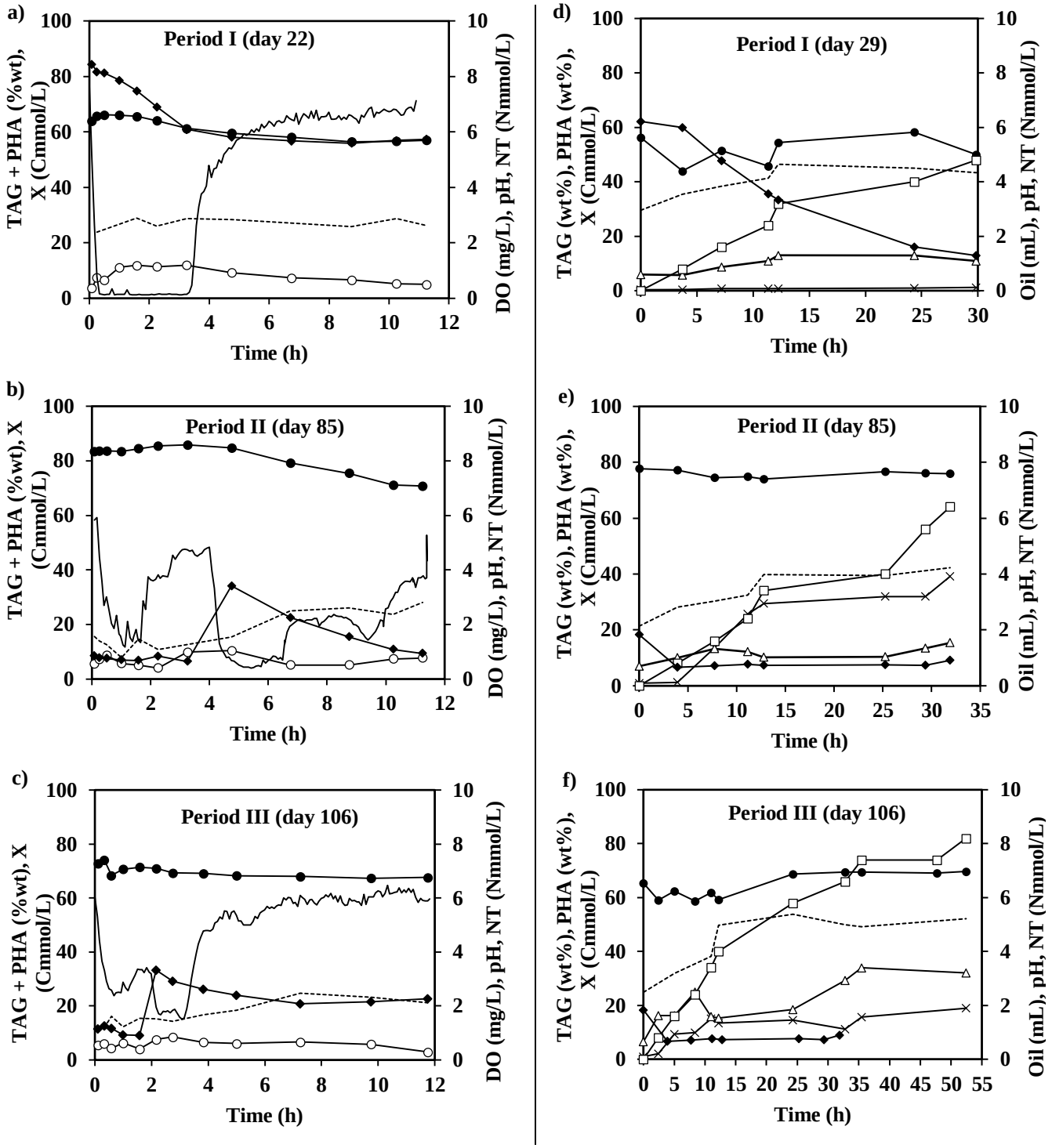

232 **Figure 1.** Characterization of three enrichment cycles (a, b, c) and three accumulation assays (d, e, f)
233 monitored in SBR-S and FBR-S, respectively. pH (●), DO (—), X (---), TN (♦), TAG + PHA (○), TAG
234 (Δ), PHA (×) and cumulative waste fish oil added (□).

235

a)	SBR – S		
Parameter	Period I (day 22)	Period II (day 85)	Period III (day 106)
% wt max.	17.0	17.4	8.5
TAG:PHA	96:4	50:50	80:20
q_{TAG} ($Cmmol_{TAG}/Cmmol_X \cdot h$)	0.063	0.017	0.028
q_{PHA} ($Cmmol_{PHA}/Cmmol_X \cdot h$)	0.002	0.042	0.020
- q_N ($Cmmol_N/Cmmol_X \cdot h$)*	0.065 – 0.000	0.004 – 0.052	0.014 – 0.020
q_X ($Cmmol_X/Cmmol_S \cdot h$) *	0.056 – 0.001	0.000 – 0.050	0.036 – 0.083
Y_{TAG} ($Cmmol_{TAG}/Cmmol_S$)	0.193	0.037	0.028
Y_{PHA} ($Cmmol_{PHA}/Cmmol_S$)	0.006	0.090	0.020
Y_X ($Cmmol_X/Cmmol_S$)*	0.181 – 0.012	0.000 – 0.363	0.098 – 0.765

b)	FBR-S		
Parameter	Period I (day 29)	Period II (day 85)	Period III (day 106)
%wt max.	13.5	54.2	50.9
TAG:PHA	94:6	28:72	63:37
q_{TAG} ($Cmmol_{TAG}/Cmmol_X \cdot h$)	0.009	0.015	0.026
q_{PHA} ($Cmmol_{PHA}/Cmmol_X \cdot h$)	0.001	0.035	0.010
Q_{TAG} ($Cmmol_{TAG}/(L \cdot h)$)	0.356	0.535	1.046
Q_{PHA} ($Cmmol_{PHA}/(L \cdot h)$)	0.021	1.239	0.409
- q_N ($Cmmol_N/Cmmol_X \cdot h$)	0.030	0.050	0.012
q_X ($Cmmol_X/Cmmol_S \cdot h$)	0.001	0.005	0.002
Y_{TAG} ($Cmmol_{TAG}/Cmmol_S$)	0.106	0.131	0.291
Y_{PHA} ($Cmmol_{PHA}/Cmmol_S$)	0.006	0.303	0.114
Y_X ($Cmmol_X/Cmmol_S$)	0.353	0.144	0.130

* Data referred to feast and famine phases: feast – famine.

Table 1. Maximum intracellular accumulation (% wt max. as a sum of TAG and PHA), maximum specific production rates (q), overall production rates (Q), and production yields (Y) determined in a) enrichment cycles (SBR-S), and b) accumulation assays (FBR-S). Fed-batch reactor (FBR-S), nitrogen (N), sequential batch reactor (SBR-S), substrate (S) , and active biomass (X).

3.1.1. Channelling lipids towards PHA accumulation

To promote the enrichment of the MMC in PHA-storing populations and hence maximise PHA production in the FBR-S, in period II C and N sources were added separately (DGL strategy) and N availability was limited to the minimum required for growth in the famine phase (Figure SI 2a) [9].

Results obtained in the SBR-S concerning the percentage of intracellular TAGs and PHAs accumulated at the end of the feast phase (Figure 2) show that the DGL strategy imposed from period II, was advantageous for PHA-storing populations even in saline environments.

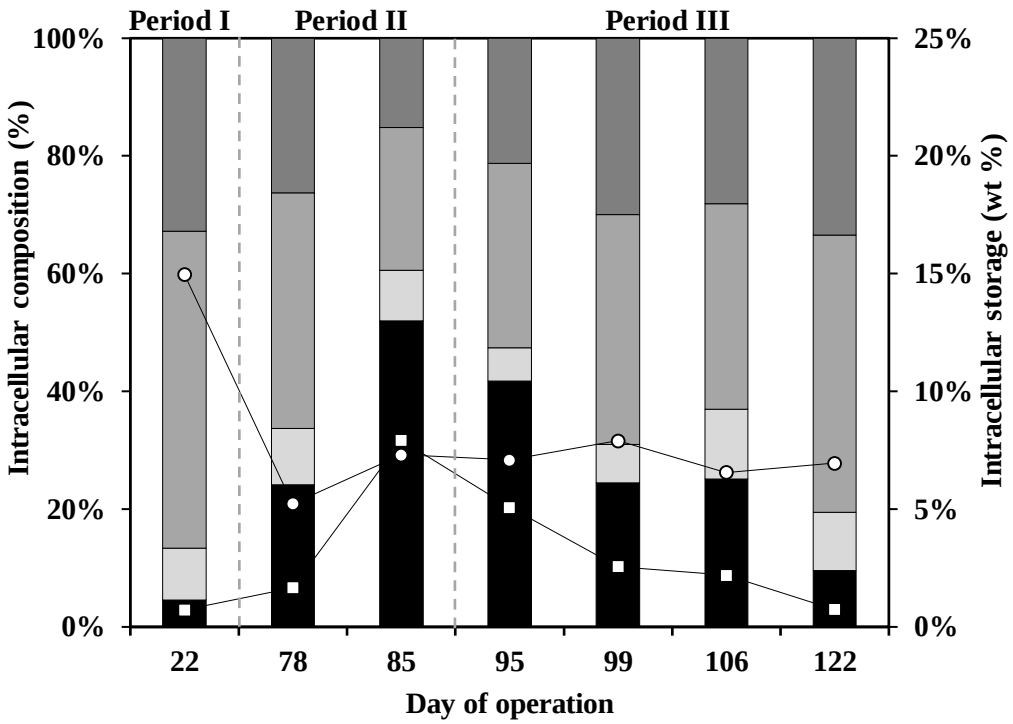

250

251 **Figure 2.** Percentages of intracellular compounds accumulated (TAG (○) and PHA (□)), and composition
252 (palmitic (□), oleic (■), linoleic (■), PHB (■)) measured at the end of the feast phase in different SBR-S
253 cycles throughout periods I – III.

254 For example, between days 22 and 85 in SBR-S, although intracellular accumulation as
255 a sum of TAGs and PHAs only increased from 17.0 to 17.4 wt %, in terms of biopolymer
256 composition, the competitive advantage of PHA-accumulators was clear (the TAG:PHA
257 ratio shifted from 96:4 to 50:50) (Table 1; Figure 2). This enrichment of the culture was
258 evidenced by the reduction of the feast/cycle ratio, which decreased from 0.31 ± 0.01 to
259 0.11± 0.03 after uncoupling (Figure SI 2b). N limitation during the feast phase led to
260 insignificant biomass production (q_X) and resulted in a larger specific PHAs accumulation
261 rate (q_{PHA}) (Table 1). The wash-out of non-storing populations that were not able to grow
262 once imposed the DGL selection strategy caused a decrease in the VSS concentration at
263 the end of the cycle between periods I and II (from 0.79 ± 0.12 to 0.63 ± 0.02 g VSS/L,
264 respectively) (Figure SI 2b).

The enrichment of the culture in PHA producers improved the accumulation capacity and productivity in the FBR-S (Figure 2). Maximum intracellular PHA accumulation and production yield increased from 0.8 wt % to 39.0 wt % and from 0.006 to 0.303 $Cmmol_{PHA}/Cmmol_{S}$, and the overall PHA production rate raised from 0.021 up to 1.239 $Cmmol_{PHA}/(L \cdot h)$, between days 29 (conventional ADF selection) and 85 (DGL selection), respectively.

Previous studies exhibited higher PHA production yields than the obtained in this study when working under concentrations of approximately 10 g NaCl/L (Table 2). Regarding the maximum storage capacity, differences were significant in comparison with pure strains but when considering MMCs and non-synthetic substrates, the results obtained in the present research work were maximum (Table 2). Besides, unlike previous authors reported [14,16,17], here it was not observed in the accumulation reactor (FBR-S) a negative effect over intracellular PHAs storage due to the osmotic stress caused by salinity. Thus, once reached the maximum accumulation, there was no intracellular PHA degradation (Figure 1e) as occurred in [14,16,17]. This result might be a consequence of the origin of the inoculum and its high degree of acclimation to saline environments before the MMC enrichment.

	Inoculum	Substrate	NaCl (g/L)	Y*	% wt max.	Reference
PHA						
	Cupriavidus necator	Acetic acid	0	0.32 (1)	61.0	[14]
			3.5	0.32	75.0	
			6.5	0.37	80.0	
			9	0.41	78.0	
			12	0.13	60.0	
			15	0.03	20.0	
	Non-acclimated activated sludge	Synthetic VFAs mixture	0	0.72(2)	53.0	[16]
			7	0.62	34.6	
			13	0.65	17.4	
			20	0.62	8.9	
	Activated sludge acclimated to salinity in the SBR	Synthetic FWFL	0	0.64 (3)	60.9	[17]
			5	0.64	50.5	
			10	0.74	52.0	
			15	0.79	42.6	
		FWFL	2.5	-	33.4	
			5	-	30.9	
			10	-	30.6	
	Sludge from a SBR located at a WWTP treating saline effluents	Waste fish oil	10	0.42 (1) 0.33 (2) 0.28 (3)	39.0	This study
TAG						
	Zygozacchorimyces rouxii	YPD	0	-	34.0	[13]
			150	-	28.3	
	Rhodosporidium toruloides	Glucose	0	0.06 (1)	42.0	[28]
			10	0.08	39.0	
			50	0.15	48.0	
			100	0.13	43.0	
	Rhodosporidium toruloides	Glucose	0	-	55.1	[11]
			5	-	62.1	
			10	-	62.2	
			15	-	62.4	
			25	-	60.6	
			40	0.18(1)	71.3	
			60	-	44.4	
	Sludge from a SBR located at a WWTP treating saline effluents	Waste fish oil	10	0.29 (1) 0.30 (2) 0.34 (3)	32.1	This study

Table 2. Influence of increasing NaCl concentrations over TAG and PHA storage in pure and mixed microbial cultures: a comparison with literature. Production yields (Y) expressed as: (1) g/g; (2) Cmmol/Cmmol; (3) g COD/g COD. Food waste fermentation leachate (FWFL), sequencing batch reactor (SBR), wastewater treatment plant (WWTP), volatile fatty acids (VFAs), yeast-peptone-dextrose medium (YPD).

3.1.2. Channelling lipids towards TAG accumulation

TAG producers present a higher tolerance to acid environments (pH 3 – 4) than PHA ones [23]. Therefore, to select TAG producers, in period III, the amount of $NaHCO_3$ buffer added in the dilution stream was decreased (Figure SI 2c).

However, the reduction of the buffer concentration under saline conditions did not cause the expected medium acidification in the famine phase that was observed in the absence of salinity [9]. The pH at the end of the cycle decreased only 0.3 units presenting high stability during the whole cycle performance. According to [24], increasing salt concentrations reduce the activity coefficient of water leading to a CO_2 solubility reduction and therefore to lower acidification of the system.

However, although it was not possible to induce in the SBR-S an environment so acidic as to favour TAG-storing populations, slightly lower pH values obtained during the feast in period III, in comparison to period II, might have affected intracellular pH regulation leading to a decrease in PHA production (Figure 2). Thus, bacteria regulate their intracellular pH (within 1 to 2 units of neutrality) by controlling the flow of protons across the membrane and when the cytoplasm becomes too acidic, protons are pumped out [25]. However, when NaCl is present in the media, Na^+ diffuses into the cells (the cell membrane is negatively charged inside and positively outside) but cells need to pump it out because it is cytotoxic [26]. Active transport of Na^+ requires proton motive force, which is generated by pumping protons inside the cytoplasm but creates an intracellular decrease of the pH that needs to be balanced. Under these conditions, the extracellular pH increases, and maintaining the intracellular pH in neutrality becomes more costly for the cell. Therefore, the intracellular pH might decrease leading to a decrease in PHA production [27]. For example, on days 85 and 106 in the SBR-S, the average pH in the feast phase was 8.4 ± 0.1 and 7.1 ± 0.2, respectively (Figures 1b, 1c.) and while TAG

storage only varied from 8.7 wt % to 6.4 wt %, intracellular PHAs decreased from 8.5 wt % to 2.1 wt%. This lower extracellular pH was also observed to affect PHAs storage in the FBR-S. Intracellular PHAs accumulation and overall PHA production rate decreased from 39.0 wt % to 18.9 wt % and from 1.239 $Cmmol_{PHA}/(L \cdot h)$ to 0.535 $Cmmol_{PHA}/(L \cdot h)$ between days 85 and 106 (average pH during the assays was 7.6 ± 0.1 and 6.5± 0.5, respectively). However, TAGs storage and overall TAG production rate increased from 15.2 wt % to 32.1 wt % and from 0.409 $Cmmol_{TAG}/(L \cdot h)$ to 1.046 $Cmmol_{TAG}/(L \cdot h)$ (Table 1; Figure 3a).

Therefore, although alkalinity reduction was not enough to acidify the medium and create a clear selective advantage for TAG producers, slightly lower pH values obtained during the feast phase could have affected intracellular pH regulation and hence PHA storage. Previous studies regarding intracellular TAG production using halotolerant strains and hydrophilic carbon sources, exhibited higher intracellular storages although lower production yields than the observed in the present research work (Table 2).

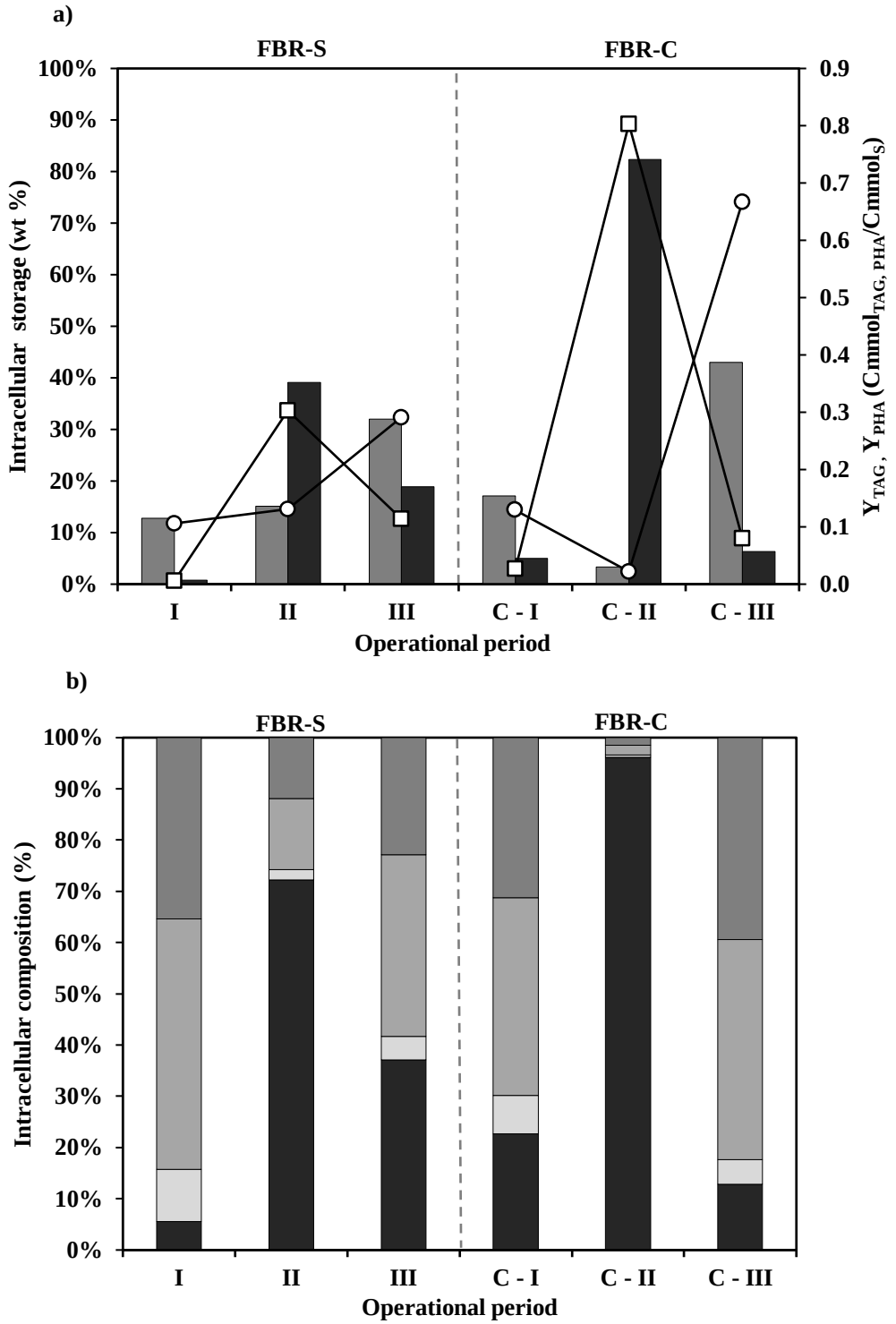

338 **Figure 3.** Comparison between FBR-S and FBR-C considering analogous operational periods (I, II, III vs
339 C-I, C-II, C-III). a) Maximum intracellular TAG (■) and PHA (■) storage and production yields (Y_{TAG} (○),
340 Y_{PHA} (□)), b) Intracellular compounds composition (palmitic (□), oleic (■), linoleic (■), PHB (■)).

341

342

3.2. Comparison with a non-saline control system

To evaluate the effect of NaCl, results obtained in this study were compared with those reached in an analogous system fed with a non-saline medium, enrichment SBR-C, and accumulation FBR-C [9]

3.2.1. Effect of osmotic stress over TAG and PHA production

Important differences were observed between SBR-C and SBR-S regarding aeration requirements and the system buffering capacity. According to DO concentration profiles, oxygen, and hence energy consumptions appeared higher in SBR-S (Figure 1) than in SBR-C [9]. Indeed, it has been postulated that higher NaCl:COD ratios lead to higher oxygen consumption rates due to additional cellular requirements [3]. On the other hand, the presence of NaCl appeared to bring stability to the pH of the system. $NaHCO_3$ addition did not need to be progressively adjusted in SBR-S (Figure SI 2c). The buffering capacity of the saline system remained stable and did not rise over time as happened in SBR-C, in which the amount of buffer added was diminished by more than 35 % during the first 50 days. This effect of NaCl over the pH could allow for a more stable and cheaper long-term operation without the need for the use of automatic control equipment. Results suggest that under high NaCl concentrations, $NaHCO_3$ buffer might not be even required to maintain the pH of the system around neutrality.

The overall activity of the MMC was also affected by osmotic stress. First, its respiration capacity was altered. Concentrations of 60 – 80 mg/L of acetic acid were measured in the media at the end of the cycle in SBR-S, which seemed to increase after N addition in the uncoupled cycle (data not shown). This demonstrates that part of the acetyl-CoA produced in the β-Oxidation of the LCFAs contained in the substrate was transformed into acetic acid and brought out of the cell instead of being channelled to the Krebs Cycle for energy generation. Secondly, it affected the overall obtained ratios of TAG and PHA

368 production, being the later the storage compound more affected. The imposition of the
369 DGL strategy under saline conditions in SBR-S (Figure 3) led to a lower degree of
370 enrichment of the culture in PHA-accumulators than in SBR-C. This could be related to
371 a possible negative effect of salinity over PHA-accumulation kinetics, which correlates
372 with the previously reported decrease of PHA production rates with NaCl concentrations
373 in the range of 5 – 20 g/L [16,17]. In the present study, on day 85 (period II), q_{PHA} was
374 0.042 $Cmmol_{PHA}/(Cmmol_X \cdot h)$ in SBR-S (10 g NaCl/L) whereas, in SBR-C (no salinity),
375 it was 0.084 $Cmmol_{PHA}/(Cmmol_X \cdot h)$ in period C-II. Besides, in SBR-S, PHAs storage
376 presented a lag phase at the beginning of the cycle and it did not start until 2 hours after
377 C source addition. However, in SBR-C, microorganisms were able to accumulate PHAs
378 from the beginning of the cycle (Figure SI 3).

379 Because of this lower degree of enrichment in SBR-S in comparison with SBR-C after
380 the uncoupling of C and N feedings, results obtained in the FBR-S (period III) were
381 substantially lower than in FBR-C (period C-III). In terms of maximum biopolymer
382 accumulation, overall production, and production yield, values of 39.0 wt % vs 82.3 wt
383 %, 1.239 $Cmmol_{PHA}/(L \cdot h)$ vs 2.225 $Cmmol_{PHA}/(L \cdot h)$, and 0.303 $Cmmol_{PHA}/Cmmol_S$ vs
384 0.803 $Cmmol_{PHA}/Cmmol_S$ were obtained, respectively. Besides, unlike what happened in
385 the non-saline system, increasing PHAs production in FBR-S after SBR-S uncoupling,
386 did not occur at the expense of TAG production (Figure 3a). This suggests that a higher
387 proportion of TAG-accumulating microorganisms remained in the MMC. In fact,
388 between days 29 and 85, TAGs production increased from 12.7 wt % (TAG:PHA ratio of
389 94:6) to 15.1 wt % (TAG:PHA ratio of 28:72). Overall, PHAs accumulation seemed more
390 affected by high salinity than TAGs accumulation (Figure 3), which correlates with
391 previously reported literature (Table 2).

Under saline conditions, preferent TAGs or PHAs accumulation was not observed as it occurred in the control system (Figure 3b). The fatty acid profile of the intracellular TAGs accumulated was very similar and proportional to that of the substrate (Table SI 1b; Figure 3b). Regarding PHAs production, no PHV was detected (Figure 3b). This was expected because no PHV was measured in the control and it was previously reported that PHV production decreases with the increase of salinity in the medium [16].

3.2.2. Effect of osmotic stress over microbial diversity

In both FBR-S and FBR-C reactors, lower diversity of *Fungi* than *Bacteria* was observed. There were 858,778 (71,565 ± 2539 per amplicon library) and 679,360 (56.613 ± 4161 per amplicon library) sequences for *Fungi* and *Bacteria*, respectively, and clustering sequences into OTUs resulted in 1,138 bacterial and 124 fungal OTUs.

The bacterial community comprised 15 different phyla distributed into 45 classes (Figure 4a, Table SI 3). 24 had a relative abundance higher than 0.05 %, and 13 composed the bacterial common core (97% of the total number of sequences). Classes *Alphaproteobacteria* and *Gammaproteobacteria* were the most abundant among the different operational periods in FBR-S. However, in FBR-C class *Gammaproteobacteria* was considerably less abundant than in the saline medium, especially in period C-II (0.30 ± 0.2 %). *Betaproteobacteria* was identified as an additional dominant class, mainly in periods C-I (33.49 ± 1.75 %) and C-III (28.48 ± 0.51 %). On the other hand, the fungal community was composed of 4 different phyla and 13 classes (Figure 4b, Table SI 4), 8 of them with a RA higher than 0.05 %.

a)

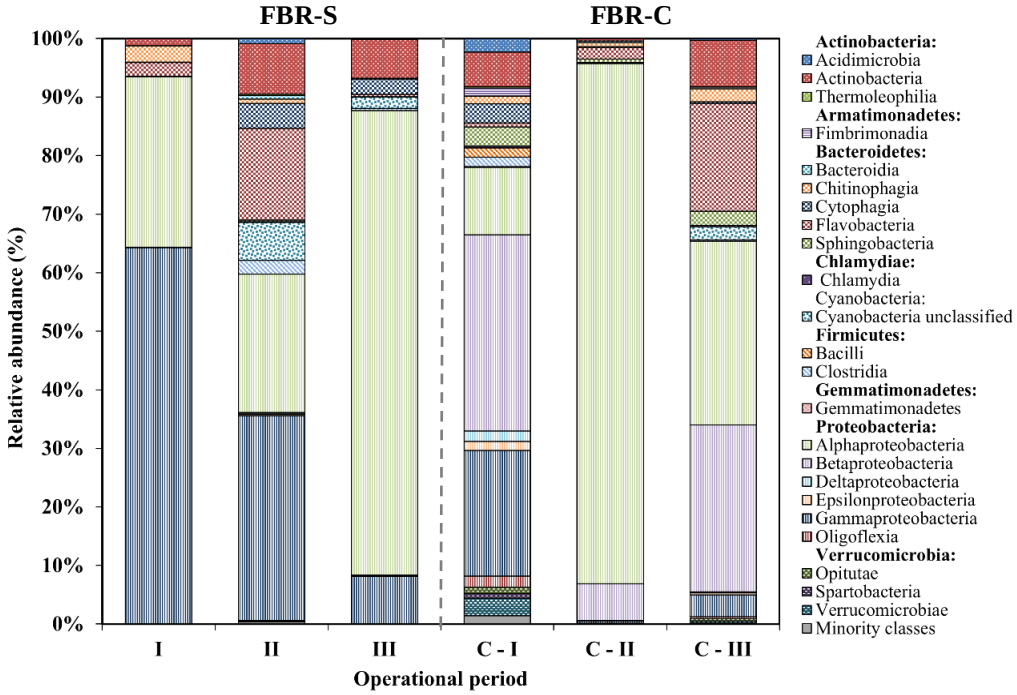

b)

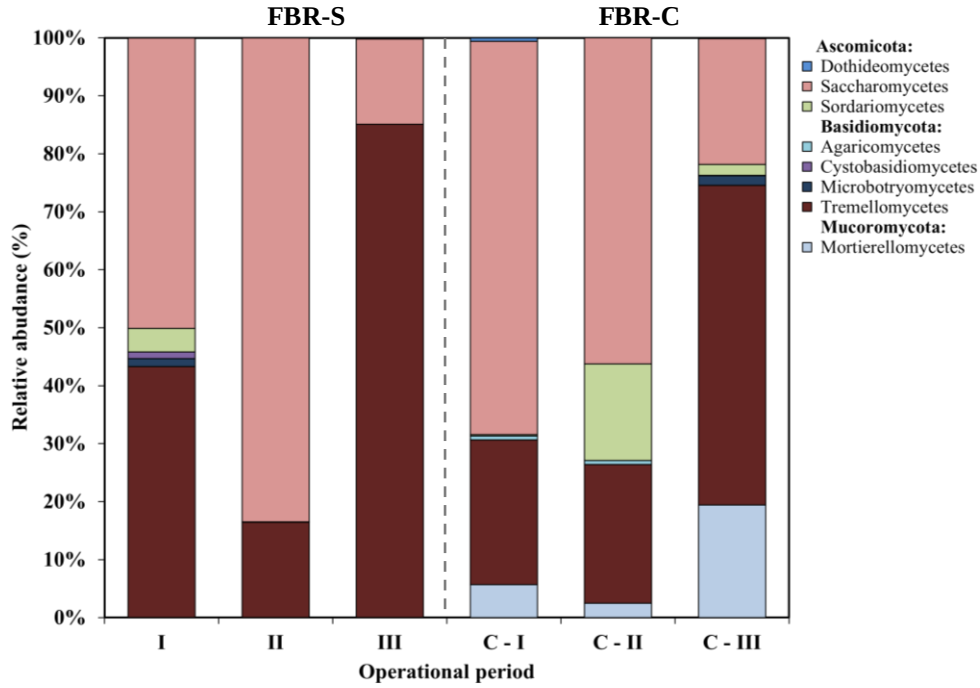

414 **Figure 4**. Structure of main bacterial (a) and fungal (b) classes (RA > 0.5%) identified by high-throughput
415 Illumina sequencing in FBR-S and FBR-C biomass samples considering analogous operational periods (I,
416 II, III vs C-I, C-II, C-III).

417

418 *Saccharomycetes* and *Tremellomycetes* were the main dominant classes in both reactors
419 throughout the distinct operational periods and the only ones comprising the fungal
420 common core (92 % of the total). According to the Kruskal-Wallis test (Conover-Iman
421 *posthoc* test), only classes *Dothideomycetes* and *Cystobasidiomycetes* (Table SI 4) from
422 FBR-S samples, and *Chlamydia* (Table SI 3) and *Agaricomycetes* from FBR-C samples
423 (Table SI 4) presented statistical differences in their RAs among periods I – III and C-I –
424 C-III, respectively. Overall, the structure of the majority of bacterial classes agreed with
425 previous research works concerning PHA accumulation in lab-scale bioreactors
426 inoculated with similar-origin inocula [29]. Also, the fungal communities found here
427 were similar to those previously described in conventional activated sludge bioreactors
428 [30].

429 Concerning the OTU level, 29 of the 1,138 bacterial OTUs (Figure 5a, Table SI 5) and 7
430 of the 124 fungal ones were dominant (RAs > 0.5 %) (Figure 5b, Table SI 6). Several
431 dominant bacterial OTUs (genera *Acidovorax* (OtuB0010), *Acinetobacter* (Otus B0003,
432 B0007 and B0008), *Comamonas* (OtuB0026), *Flavobacterium* (OtuB0013), *Lysobacter*
433 (OtuB0022), and *Pseudomonas* (OtuB0024), *Rhizobium* (Otus B0014 and B0015)) were
434 previously identified as able to accumulate PHAs [21,31–34]. Besides, different bacterial
435 (genera *Acinetobacter* (Otus B0003, B0007 and B0008), *Gordonia* (OtuB0012) and
436 *Pseudomonas* (OtuB0024)) and fungal (yeasts *Mortierella* (OtuF0007) and *Yarrowia*
437 (OtuF0009)) ones were previously proposed as TAG-storing microorganisms [4,35–38].

438

439

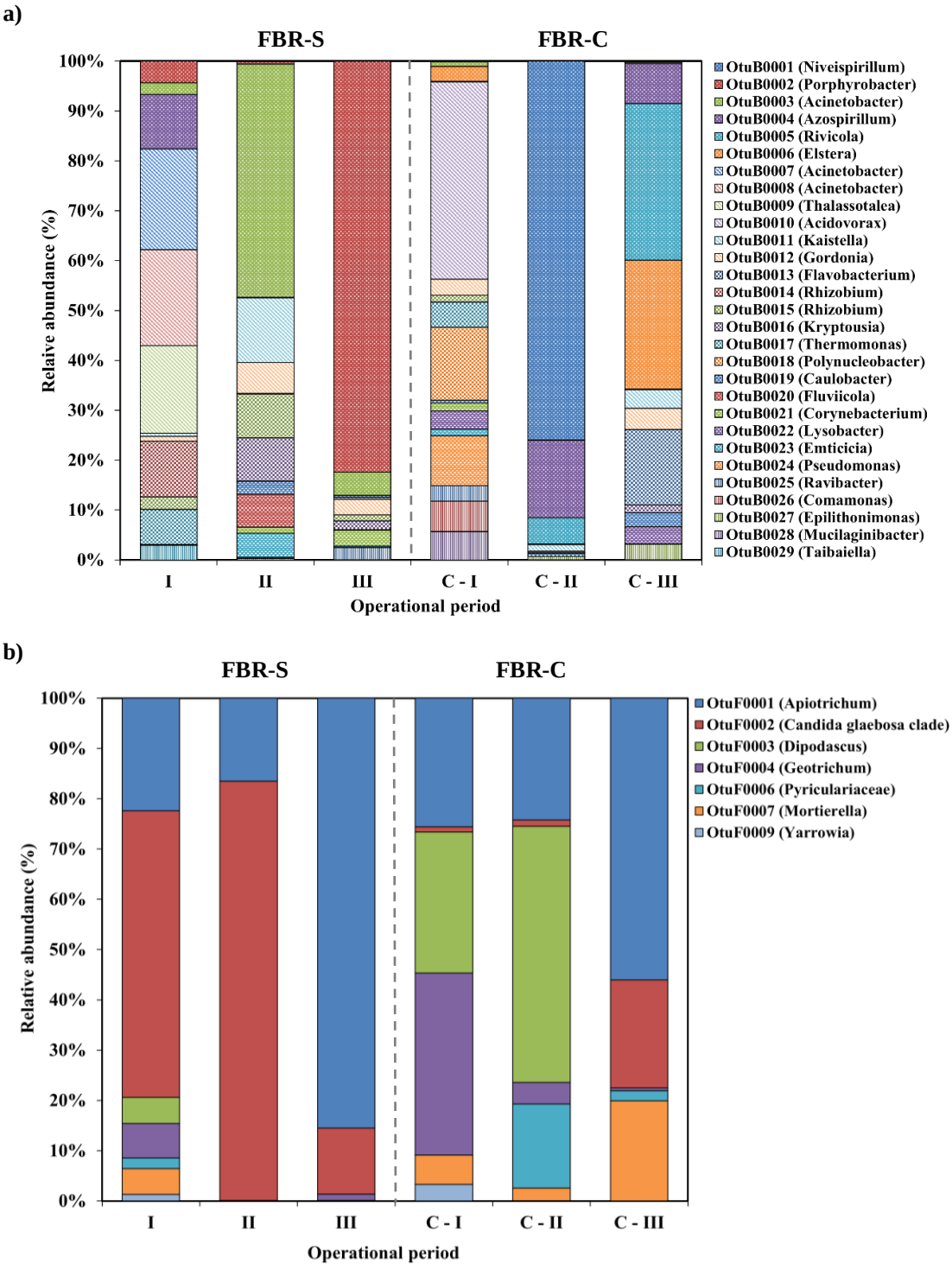

Figure 5. Relative abundance of the main bacterial (a) and fungal (b) OTUs (RA > 0.5%) identified by high-throughput Illumina sequencing in FBR-S and FBR-C biomass samples considering analogous operational periods (I, II, III vs C-I, C-II, C-III).

Both FBR-S and FBR-C microbial communities presented important differences in each reactor between the periods studied as a consequence of the operational conditions and selective pressures implemented, which modulated their structure. Only the bacterial groups OtuB0006 (*Elstera*), OtuB0017 (*Thermomonas*), OtuB0022 (*Lysobacter*), and OtuB0020 (*Fluviicola*) did not present statistical differences over time in both FBR-S and FBR-C (Table SI 4). Similarly, all the fungal OUT's RAs found in FBR-C were statistically different among periods C-I – C-III, and only the RAs of OtuF0003 (*Dipodascus*) did not show differences over time in FBR-S (Table SI 5).

However, the hierarchical clustering analyses performed to evaluate the global effect of salinity in the bacterial and fungal OTUs (Figure SI 4) showed that for both communities, salinity was a driver stronger than the operational period. Thus, the RAs of the dominant OTUs for FBR-S and FBR-C were separated according to their origin (except for the bacterial community of FBR-S in period III, in which RAs were separated according to the operational period) evidencing that NaCl stress specifically modulates the structure of the dominant OTUs, as previous authors observed [39].

According to the Mann-Whitney test, independently of the sampling period, high salinity negatively affected the presence of OtuB0005 (*Rivicola*), OtuB0006 (*Elstera*), OtuB0022 (*Lysobacter*) (Figure 5a, Table SI 4), NaCl sensitive bacterial genera [40,41] that have not been identified yet as TAG or PHA-storing populations. Nonetheless, all of them reached the highest relative abundance in period C-III of FBR-C (26.21 ± 0.63 %, 21.54 ± 0.03 %, and 2.87 ± 0.08 % for *Rivicola*, *Elstera* and *Lysobacter* respectively), in which the maximum intracellular TAG accumulation was obtained (Figure 3). Concerning the *Eukarya* domain, osmotic stress hindered the presence of OtuF0003 (*Dipodascus*) and Otu0007 (*Mortierella*) (Figure 5b, Table SI 5). *Dipodascus* is a yeast without a TAG accumulation trait [42] which relative abundance decreased from 50.13 ± 0.21 % to non-

detected between periods C-II (highest PHA accumulation) and C-III (highest TAG accumulation (Figure 3). *Mortierella* is an oleaginous mould which accumulation capacity was reported to be negatively correlated to NaCl [43]. It presented a relative abundance of 19.41 ± 3.10 % in period C-III in FBR-C (highest TAG production, Figure 3), whereas in FBR-S it was only detected in period II with a RA lower than 0.05 %.

On the other hand, salinity stimulated the development of OtuB0002 (*Porphyrobacter*), OtuB0003 (*Acinetobacter*), OtuB0015 (*Rhizobium*), OtuB0016 (*Kryptousia*), OtuB0021 (*Corynebacterium*), OtuB0029 (*Taibaiella*), OtuB0027 (*Epilithonimonas*), and OtuF0002 (*Candida glaebosa* clade) (Tables SI 4 and SI 5). *Porphyrobacter* was previously described as halotolerant [44] and although, until the date, it was not identified as a TAG or PHA-storing microorganism its relative abundance notably increased when the highest TAG storage was reached in FBR-S (Figure 3, Figure 5a). *Acinetobacter* is an osmotolerant bacterium (Hrenovic and Ivankovic, 2009) identified as capable of producing PHAs [46] and TAGs [47]. Its relative abundance notably increased in FBR-S between periods I and II (highest PHA production) whereas in period III became very scarce. *Rhizobium* was reported to survive under salt stress conditions [48] and, despite being a PHA-storing microorganism [49], its presence was only observed in period I in FBR-S (lowest intracellular PHA storage, Figure 3). *Kryptousia* was developed after the SBR-S uncoupling and its relations to NaCl stress or biopolymer production are still unknown. *Corynebacterium*, with a scarce presence in FBR-S (highest RA of 2.88 ± 0.80 % in period III), can store amino-acids in response to osmotic stress although it is not a TAG or PHA synthesizer [50]. *Taibaiella* (highest RA of 2.67 ± 0.10 %) was previously characterized as slightly NaCl tolerant, [51] but to the best of the author´s knowledge, is not a TAG or PHA-storing microorganism. *Candida glaebosa* clade, affine to hypersaline environments [52] presented a high abundance in FBR-S throughout the different

494 operational periods reaching its maximum in period II (82.92 ± 1.32). The TAG
495 accumulation capacity in members of the current *Candida* genus has been previously
496 characterized [53]. However, the uncertain position of the members of this clade inside
497 the family *Debaryomycetaceae* hinders their assign within the group of oleaginous yeasts
498 [54].

499

500 **4. CONCLUSIONS**

501 The use of saline water (10 g NaCl/L) for dilution in a two-stage process for TAGs and
502 PHAs recovery from industrial waste fish oil appeared feasible according to the results
503 obtained in this study. However, further optimization focused on the adaptation of the
504 imposed selective pressures to the effect caused by salinity, would allow for the obtention
505 of more competitive outcomes.

506 • When PHAs were the main storage compound (TAG:PHA = 28:72), 39.0 wt %
507 PHA was accumulated yielding 0.303 $Cmmol_{PHA}/Cmmol_{S}$. On the other hand,
508 when TAG producers dominated (TAG:PHA = 63:37), a maximum of 32.1 wt %
509 TAG was observed yielding 0.291 $Cmmol_{TAG}/Cmmol_{S.}$

510 • The selective pressures imposed in the enrichment stage to maximize preferent
511 TAGs or PHAs production in the accumulation reactor seemed less efficient when
512 NaCl was present in the medium.

513 • PHA producers appeared more sensitive to salt and although the DGL strategy
514 favoured their development, the culture needed to be further enriched to increase
515 specificity. In the case of TAGs, a more severe medium acidification might be
516 needed in saline conditions to create a clear selective advantage for TAG
517 producers.

- Salinity was observed to be the main factor influencing the structure of both bacterial and fungal communities. Several OTUs presented a high relative abundance in the presence of salinity, some of them previously identified as TAG or PHA-storing microorganisms (*Acinetobacter*, *Rhizobium* and *Candida glaebosa* clade).

5. ACKNOWLEDGMENTS

This research was supported by the Spanish Government (AEI) through the TREASURE project [CTQ2017-83225-C2-1-R]. Lucía Argiz is a Xunta de Galicia fellow (2019), [ED 481A-2019/083]. The authors belong to the Galician Competitive Research Group GRC ED431C 2017/29 and all these programs are co-funded by the FEDER (EU).

6. REFERENCES

[1] A. Monteiro, D. Paquincha, F. Martins, R.P. Queirós, J.A. Saraiva, J. Švarc-Gajić, N. Nastić, C. Delerue-Matos, A.P. Carvalho, Liquid by-products from fish canning industry as sustainable sources of ω3 lipids, J. Environ. Manage. 219 (2018) 9–17. https://doi.org/10.1016/j.jenvman.2018.04.102.

[2] K.B. Chipasa, K. Mędrzycka, Behavior of lipids in biological wastewater treatment processes, J. Ind. Microbiol. Biotechnol. 33 (2006) 635–645. https://doi.org/10.1007/s10295-006-0099-y.

[3] R.O. Cristóvão, V.M.S. Pinto, R.J.E. Martins, J.M. Loureiro, R.A.R. Boaventura, Assessing the influence of oil and grease and salt content on fish canning wastewater biodegradation through respirometric tests, J. Clean. Prod. 127 (2016) 343–351. https://doi.org/10.1016/j.jclepro.2016.04.057.

[4] J. Tamis, D.Y. Sorokin, Y. Jiang, M.C.M. Van Loosdrecht, R. Kleerebezem, Lipid recovery from a vegetable oil emulsion using microbial enrichment cultures, Biotechnol. Biofuels. 8 (2015) 1–11. https://doi.org/10.1186/s13068-015-0228-9.

[5] D. Van Thuoc, D.N. My, T.T. Loan, K. Sudesh, Utilization of waste fish oil and glycerol as carbon sources for polyhydroxyalkanoate production by Salinivibrio sp. M318, Int. J. Biol. Macromol. 141 (2019) 885–892. https://doi.org/10.1016/j.ijbiomac.2019.09.063.

[6] K. Sangkharak, N. Paichid, T. Yunu, S. Klomklao, P. Prasertsan, Utilisation of tuna condensate waste from the canning industry as a novel substrate for polyhydroxyalkanoate production, Biomass Convers. Biorefinery. (2020). https://doi.org/10.1007/s13399-019-00581-4.

[7] S. Campanari, F.A. E Silva, L. Bertin, M. Villano, M. Majone, Effect of the organic loading rate on the production of polyhydroxyalkanoates in a multi-stage process aimed at the valorization of olive oil mill wastewater, Int. J. Biol. Macromol. 71 (2014) 34–41. https://doi.org/10.1016/j.ijbiomac.2014.06.006.

[8] K. Gobi, V.M. Vadivelu, Aerobic dynamic feeding as a strategy for in situ accumulation of polyhydroxyalkanoate in aerobic granules, Bioresour. Technol. 161 (2014) 441–445. https://doi.org/10.1016/j.biortech.2014.03.104.

[9] L. Argiz, R. González-Cabaleiro, Á. Val del Río, J. González-López, A. Mosquera-Corral, A novel strategy for triacylglycerides and polyhydroxyalkanoates production using waste lipids, Sci. Total Environ. 763 (2021). https://doi.org/10.1016/j.scitotenv.2020.142944.

[10] N. Singh, B. Choudhury, Valorization of food-waste hydrolysate by Lentibacillus salarius NS12IITR for the production of branched chain fatty acid enriched lipid with potential application as a feedstock for improved biodiesel, Waste Manag. 94 (2019) 1–9. https://doi.org/10.1016/j.wasman.2019.05.033.

[11] S.S. Tchakouteu, N. Kopsahelis, A. Chatzifragkou, O. Kalantzi, N.G. Stoforos, A.A. Koutinas, G. Aggelis, S. Papanikolaou, Rhodosporidium toruloides cultivated in NaCl-enriched glucose-based media: Adaptation dynamics and lipid production, Eng. Life Sci. 17 (2017) 237–248. https://doi.org/10.1002/elsc.201500125.

[12] G. Venkata Subhash, S. Venkata Mohan, Lipid accumulation for biodiesel production by oleaginous fungus Aspergillus awamori: Influence of critical factors, Fuel. 116 (2014) 509–515. https://doi.org/10.1016/j.fuel.2013.08.035.

[13] K. Hosono. Effect of salt stress on lipid composition and membrane fluidity of the salt- tolerant yeast Zygosaccharomyces rouxii, (1992) 91–96.

[14] P. Passanha, G. Kedia, R.M. Dinsdale, A.J. Guwy, S.R. Esteves, The use of NaCl addition for the improvement of polyhydroxyalkanoate production by Cupriavidus necator, Bioresour. Technol. 163 (2014) 287–294. https://doi.org/10.1016/j.biortech.2014.04.068.

[15] P. Sedlacek, E. Slaninova, M. Koller, J. Nebesarova, I. Marova, V. Krzyzanek, S. Obruca, PHA granules help bacterial cells to preserve cell integrity when exposed to sudden osmotic imbalances, N. Biotechnol. 49 (2019) 129–136. https://doi.org/10.1016/j.nbt.2018.10.005.

[16] T. Palmeiro-Sánchez, A. Fra-Vázquez, N. Rey-Martínez, J.L. Campos, A. Mosquera-Corral, Transient concentrations of NaCl affect the PHA accumulation in mixed microbial culture, J. Hazard. Mater. 306 (2016) 332–339. https://doi.org/10.1016/j.jhazmat.2015.12.032.

[17] Q. Wen, Y. Ji, Y. Hao, L. Huang, Z. Chen, M. Sposob, Effect of sodium chloride on polyhydroxyalkanoate production from food waste fermentation leachate under different organic loading rate, Bioresour. Technol. 267 (2018) 133–140. https://doi.org/10.1016/j.biortech.2018.07.036.

[18] P. Taylor, M. Soto, M.C. Veiga, R. Méndez, J.M. Lema, Semi - micro C . O . D . determination method for high - salinity wastewater SEMI-MICRO C . O . D . DETERMINATION METHOD FOR HIGH-SALINITY WASTEWATER, Environ. Technol. Lett. (1989) 37–41. https://doi.org/10.1080/09593338909384770.

[19] G.J.F. Smolders, J. van der Meij, M.C.M. van Loosdrecht, J.J. Heijnen, Stoichiometric model of the aerobic metabolism of the biological phosphorus removal process, Biotechnol. Bioeng. 44 (1994) 837–848. https://doi.org/10.1002/bit.260440709.

[20] S. Takahashi, J. Tomita, K. Nishioka, T. Hisada, M. Nishijima, Development of a prokaryotic universal primer for simultaneous analysis of Bacteria and Archaea using next-generation sequencing, PLoS One. 9 (2014). https://doi.org/10.1371/journal.pone.0105592.

607 [21] C.M. Liu, S. Kachur, M.G. Dwan, A.G. Abraham, M. Aziz, P.R. Hsueh, Y.T.
608 Huang, J.D. Busch, L.J. Lamit, C.A. Gehring, P. Keim, L.B. Price, FungiQuant: a
609 broad-coverage fungal quantitative real-time PCR assay., BMC Microbiol. 12
610 (2012). https://doi.org/10.1186/1471-2180-12-255.

611 [22] D. Dionisi, M. Majone, G. Vallini, S. Di Gregorio, M. Beccari, Effect of the
612 Applied Organic Load Rate on Biodegradable Polymer Production by Mixed
613 Microbial Cultures in a Sequencing Batch Reactor, (2005).
614 https://doi.org/10.1002/bit.20683.

615 [23] F. Santamauro, F.M. Whiffin, R.J. Scott, C.J. Chuck, Low-cost lipid production by
616 an oleaginous yeast cultured in non-sterile conditions using model waste resources,
617 Biotechnol. Biofuels. 7 (2014) 1–11. https://doi.org/10.1186/1754-6834-7-34.

618 [24] Q. Sun, H. Tian, Z. Li, X. Guo, A. Liu, L. Yang, Solubility of CO2 in water and
619 NaCl solution in equilibrium with hydrate. Part I: Experimental measurement,
620 Fluid Phase Equilib. 409 (2016) 131–135.
621 https://doi.org/10.1016/j.fluid.2015.09.033.

622 [25] D. White, J. Drummond, C. Fuqua, N. York, The Physiology and Biochemistry of
623 Prokaryotes. Fourth edicion

624 [26] E. Padan, E. Bibi, M. Ito, T.A. Krulwich, Alkaline pH homeostasis in bacteria:
625 New insights, Biochim. Biophys. Acta - Biomembr. 1717 (2005) 67–88.
626 https://doi.org/10.1016/j.bbamem.2005.09.010.

627 [27] G. Montiel-Jarillo, J. Carrera, M.E. Suárez-Ojeda, Enrichment of a mixed
628 microbial culture for polyhydroxyalkanoates production: Effect of pH and N and
629 P concentrations, Sci. Total Environ. 583 (2017) 300–307.
630 https://doi.org/10.1016/j.scitotenv.2017.01.069.

631 [28] G. Singh, A. Jawed, D. Paul, K.K. Bandyopadhyay, A. Kumari, S. Haque,
632 Concomitant production of lipids and carotenoids in Rhodosporidium toruloides
633 under osmotic stress using response surface methodology, Front. Microbiol. 7
634 (2016) 1–13. https://doi.org/10.3389/fmicb.2016.01686.

635 [29] E. Korkakaki, M. Mulders, A. Veeken, R. Rozendal, M.C.M. van Loosdrecht, R.
636 Kleerebezem, PHA production from the organic fraction of municipal solid waste
637 (OFMSW): Overcoming the inhibitory matrix, Water Res. 96 (2016) 74–83.

https://doi.org/10.1016/j.watres.2016.03.033.

[30] L. Niu, Y. Li, L. Xu, P. Wang, W. Zhang, C. Wang, W. Cai, L. Wang, Ignored fungal community in activated sludge wastewater treatment plants: diversity and altitudinal characteristics, Environ. Sci. Pollut. Res. 24 (2017) 4185–4193. https://doi.org/10.1007/s11356-016-8137-4.

[31] D. Inoue, Y. Suzuki, T. Uchida, J. Morohoshi, K. Sei, Polyhydroxyalkanoate production potential of heterotrophic bacteria in activated sludge, J. Biosci. Bioeng. 121 (2016) 47–51. https://doi.org/10.1016/j.jbiosc.2015.04.022.

[32] F. Morgan-Sagastume, Characterisation of open, mixed microbial cultures for polyhydroxyalkanoate (PHA) production, Rev. Environ. Sci. Biotechnol. 15 (2016) 593–625. https://doi.org/10.1007/s11157-016-9411-0.

[33] F. Morgan-Sagastume, M. Hjort, D. Cirne, F. Gérardin, S. Lacroix, G. Gaval, L. Karabegovic, T. Alexandersson, P. Johansson, A. Karlsson, S. Bengtsson, M. V. Arcos-Hernández, P. Magnusson, A. Werker, Integrated production of polyhydroxyalkanoates (PHAs) with municipal wastewater and sludge treatment at pilot scale, Bioresour. Technol. 181 (2015) 78–89. https://doi.org/10.1016/j.biortech.2015.01.046.

[34] D. Li, F. Yin, X. Ma, Towards biodegradable polyhydroxyalkanoate production from wood waste: Using volatile fatty acids as conversion medium, Bioresour. Technol. 299 (2020) 122629. https://doi.org/10.1016/j.biortech.2019.122629.

[35] H.M. Alvarez, Triacylglycerol and wax ester-accumulating machinery in prokaryotes, Biochimie. 120 (2016) 28–39. https://doi.org/10.1016/j.biochi.2015.08.016.

[36] M. Cea, N. Sangaletti-Gerhard, P. Acuña, I. Fuentes, M. Jorquera, K. Godoy, F. Osses, R. Navia, Screening transesterifiable lipid accumulating bacteria from sewage sludge for biodiesel production, Biotechnol. Reports. 8 (2015) 116–123. https://doi.org/10.1016/j.btre.2015.10.008.

[37] M. Lopes, A.S. Gomes, C.M. Silva, I. Belo, Microbial lipids and added value metabolites production by Yarrowia lipolytica from pork lard, J. Biotechnol. 265 (2018) 76–85. https://doi.org/10.1016/j.jbiotec.2017.11.007.

[38] A.D. Jones, K.L. Boundy-Mills, G.F. Barla, S. Kumar, B. Ubanwa, V. Balan,

669 Microbial lipid alternatives to plant lipids, 2019. https://doi.org/10.1007/978-1-
670 4939-9484-7_1.

671 [39] A. Rodriguez-Sanchez, J.C. Leyva-Diaz, J.M. Poyatos, J. Gonzalez-Lopez,
672 Influent salinity conditions affect the bacterial communities of biofouling in hybrid
673 MBBR-MBR systems, J. Water Process Eng. 30 (2019) 100650.
674 https://doi.org/10.1016/j.jwpe.2018.07.001.

675 [40] S.Y. Sheu, J.C. Chen, C.C. Young, W.M. Chen, Rivicola pingtungensis gen. nov.,
676 sp. nov., a new member of the family Neisseriaceae isolated from a freshwater
677 river, Int. J. Syst. Evol. Microbiol. 64 (2014) 2009–2016.
678 https://doi.org/10.1099/ijs.0.055285-0.

679 [41] H. Cai, Y. Zeng, Y. Wang, H. Jiang, Elstera cyanobacteriorum sp. nov., a novel
680 bacterium isolated from cyanobacterial aggregates in a eutrophic lake, Int. J. Syst.
681 Evol. Microbiol. 67 (2017) 4272–4275. https://doi.org/10.1099/ijsem.0.002308.

682 [42] S. Kunthiphun, P. Chokreansukchai, P. Hondee, S. Tanasupawat, A. Savarajara,
683 Diversity and characterization of cultivable oleaginous yeasts isolated from
684 mangrove forests, World J. Microbiol. Biotechnol. 34 (2018) 0.
685 https://doi.org/10.1007/s11274-018-2507-7.

686 [43] S.Y. Ho, F. Chen, Lipid characterization of Mortierella alpina grown at different
687 NaCl concentrations, J. Agric. Food Chem. 56 (2008) 7903–7909.
688 https://doi.org/10.1021/jf801404y.

689 [44] K. Furuhata, A. Edagawa, H. Miyamoto, Y. Kawakami, M. Fukuyama,
690 Porphyrobacter colymbi sp. nov. isolated from swimming pool water in Tokyo,
691 Japan, J. Gen. Appl. Microbiol. 59 (2013) 245–250.
692 https://doi.org/10.2323/jgam.59.245.

693 [45] J. Hrenovic, T. Ivankovic, Survival of Escherichia coli and Acinetobacter junii at
694 various concentrations of sodium chloride, EurAsian J. Biosci. 151 (2009) 144–
695 151. https://doi.org/10.5053/ejobios.2009.3.0.18.

696 [46] M.A. Schembri, R.C. Bayly, J.K. Davies, Phosphate concentration regulates
697 transcription of the Acinetobacter polyhydroxyalkanoic acid biosynthetic genes, J.
698 Bacteriol. 177 (1995) 4501–4507. https://doi.org/10.1128/jb.177.15.4501-
699 4507.1995.

[47] K. Salcedo-Vite, J.C. Sigala, D. Segura, G. Gosset, A. Martinez, Acinetobacter baylyi ADP1 growth performance and lipid accumulation on different carbon sources, Appl. Microbiol. Biotechnol. 103 (2019) 6217–6229. https://doi.org/10.1007/s00253-019-09910-z.

[48] J. Nogales, R. Campos, H. BenAbdelkhalek, J. Olivares, C. Lluch, J. Sanjuan, Rhizobium tropici genes involved in free-living salt tolerance are required for the establishment of efficient nitrogen-fixing symbiosis with Phaseolus vulgaris, Mol. Plant-Microbe Interact. 15 (2002) 225–232. https://doi.org/10.1094/MPMI.2002.15.3.225.

[49] O. V. Kosmachevskaya, E. V. Osipov, T. Van Chi, P.T.T. Mai, A.F. Topunov, Effect of Cultivation Conditions on Poly(3-hydroxybutyrate) Synthesis by Nodule Bacteria Rhizobium phaseoli, Appl. Biochem. Microbiol. 56 (2020) 64–71. https://doi.org/10.1134/S000368382001010X.

[50] J. Plassmeier, Y. Li, C. Rueckert, A.J. Sinskey, Metabolic engineering Corynebacterium glutamicum to produce triacylglycerols, Metab. Eng. 33 (2016) 86–97. https://doi.org/10.1016/j.ymben.2015.11.002.

[51] I. Szabó, S. Szoboszlay, A. Táncsics, S.G. Szerdahelyi, Szűcs, J. Radó, T. Benedek, L. Szabó, H.G. Daood, M. Cserháti, B. Kriszt, Taibaiella coffeisoli sp. nov., isolated from the soil of a coffee plantation, Int. J. Syst. Evol. Microbiol. 66 (2016) 1627–1632. https://doi.org/10.1099/ijsem.0.000873.

[52] A.W.F. Duarte, I. Dayo-Owoyemi, F.S. Nobre, F.C. Pagnocca, L.C.S. Chaud, A. Pessoa, M.G.A. Felipe, L.D. Sette, Taxonomic assessment and enzymes production by yeasts isolated from marine and terrestrial Antarctic samples, Extremophiles. 17 (2013) 1023–1035. https://doi.org/10.1007/s00792-013-0584-y.

[53] A. Chattopadhyay, R. Singh, M. Mitra, A.K. Das, M.K. Maiti, Identification and functional characterization of a lipid droplet protein CtLDP1 from an oleaginous yeast Candida tropicalis SY005, Biochim. Biophys. Acta - Mol. Cell Biol. Lipids. 1865 (2020) 158725. https://doi.org/10.1016/j.bbalip.2020.158725.

[54] H.M. Daniel, M.A. Lachance, C.P. Kurtzman, On the reclassification of species assigned to Candida and other anamorphic ascomycetous yeast genera based on phylogenetic circumscription, Antonie van Leeuwenhoek, Int. J. Gen. Mol.

732 Microbiol. 106 (2014) 67–84. https://doi.org/10.1007/s10482-014-0170-z.

733

734

Open-culture biotechnological process for triacylglycerides and polyhydroxyalkanoates recovery from industrial waste fish oil under saline conditions

Lucía Argiz[a*], Rebeca González-Cabaleiro[b], David Correa-Galeote[c], Ángeles Val del Río[a], Anuska Mosquera Corral[a]

[a] CRETUS Institute, Department of Chemical Engineering, Universidade de Santiago de Compostela, 15782 Santiago de Compostela, Galicia, Spain

[b] Department of Biotechnology, Delft University of Technology, Van der Maasweg 9, 2629 HZ Delft, the Netherlands.

[c] Department of Microbiology and Institute of Water Research, Universidad de Granada, Granada, Spain.

* Corresponding author: luciaargiz.montes@usc.es

Figure SI 1. Configuration of the SBR-S operational cycles during periods I – III.

a) Coupled system configuration (period I)

Feeding [1]			
Aeration			
Withdrawal			
Time (min)	**5**	**708**	**7**

[1] 2 mL C (waste fish oil) & 2 L of a nutrient solution containing N.

b) Uncoupled system configuration (periods II and III)

Feeding [2]					
Aeration					
Feeding [3]					
Withdrawal					
Time (min)	**5**	**120 – 180**	**5**	**523 - 583**	**7**

[2] 2 mL C (waste fish oil) & 2 L of a nutrients solution without N; [3] 20 mL of a N solution.

Figure SI 2. Evolution of different operational parameters in SBR-S. Concentrations of a) TN in the feeding (♦), and TN at the end of the cycle (♦); b) feast phase length considering accumulation + growth (×), feast phase length considering only accumulation (●) and VSS concentration (—); c) pH at the end of the cycle (●) and $NaHCO_3$ concentration in the feeding (▲).

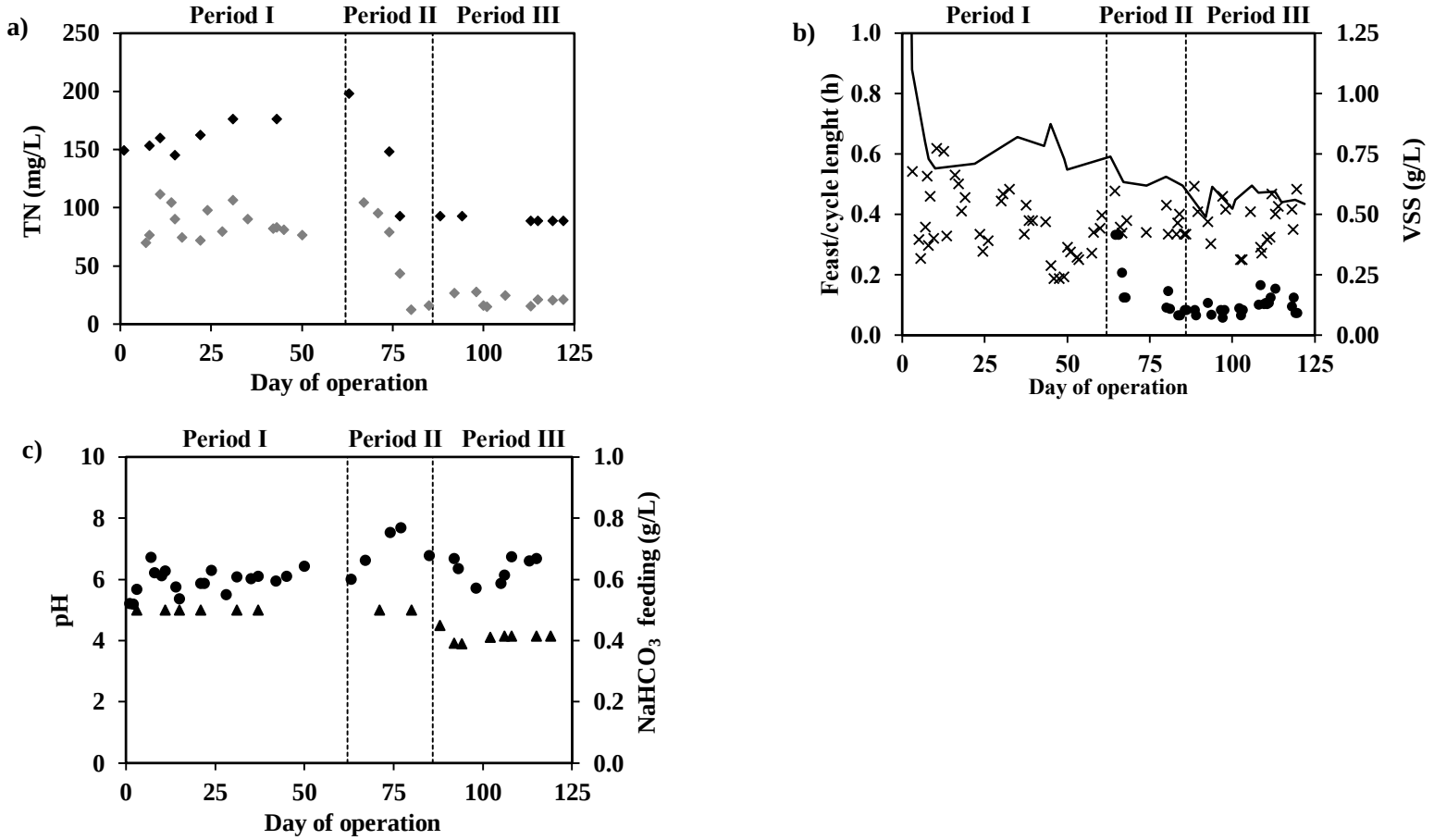

Figure SI 3. Intracellular PHA accumulation in saline (SBR-S) and non- saline (SBR-C) enrichment reactors operated under the DGL strategy (uncoupled C and N addition).

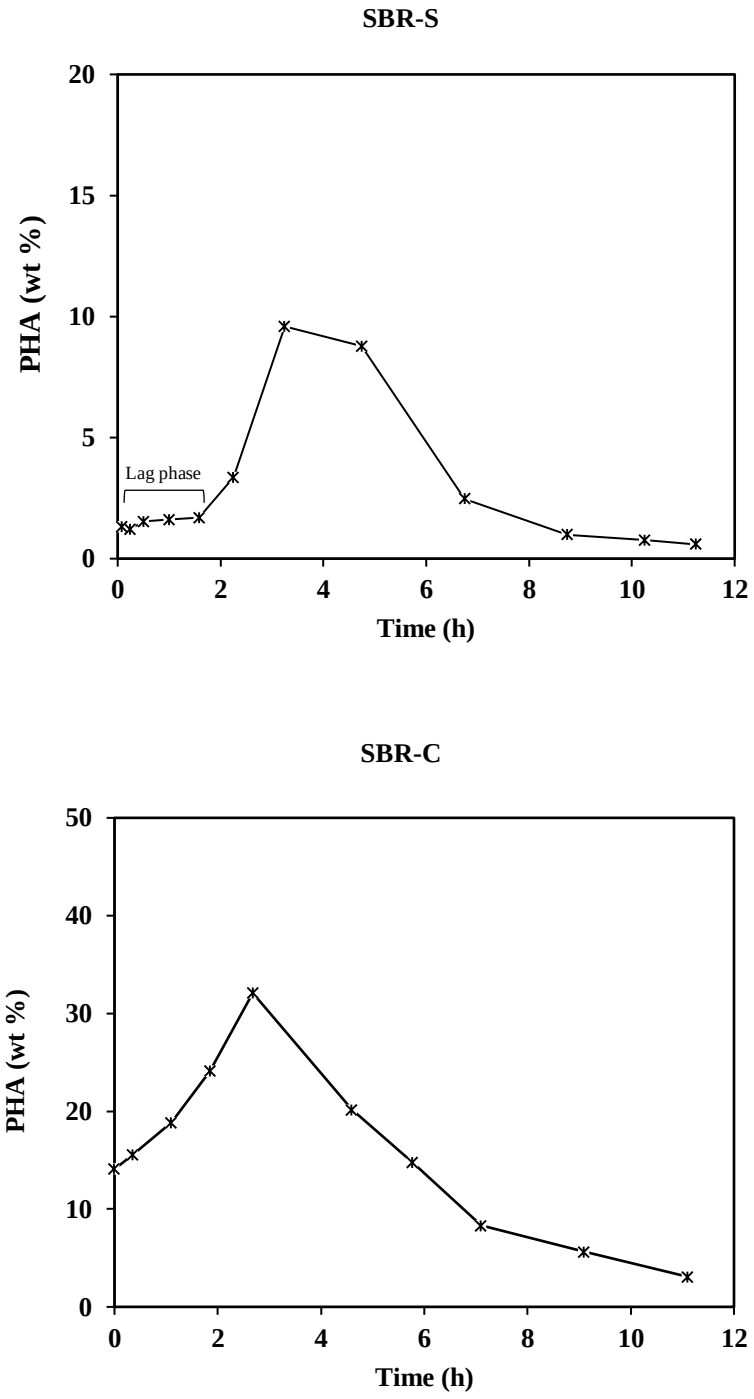

Figure SI 4. Heatmap of the average clustering of the relative abundance of the main bacterial (a) and fungal (b) OTUs identified in the DNA isolated from accumulation saline and non-saline bioreactors (FBR-S and FBR-C, respectively).

a)

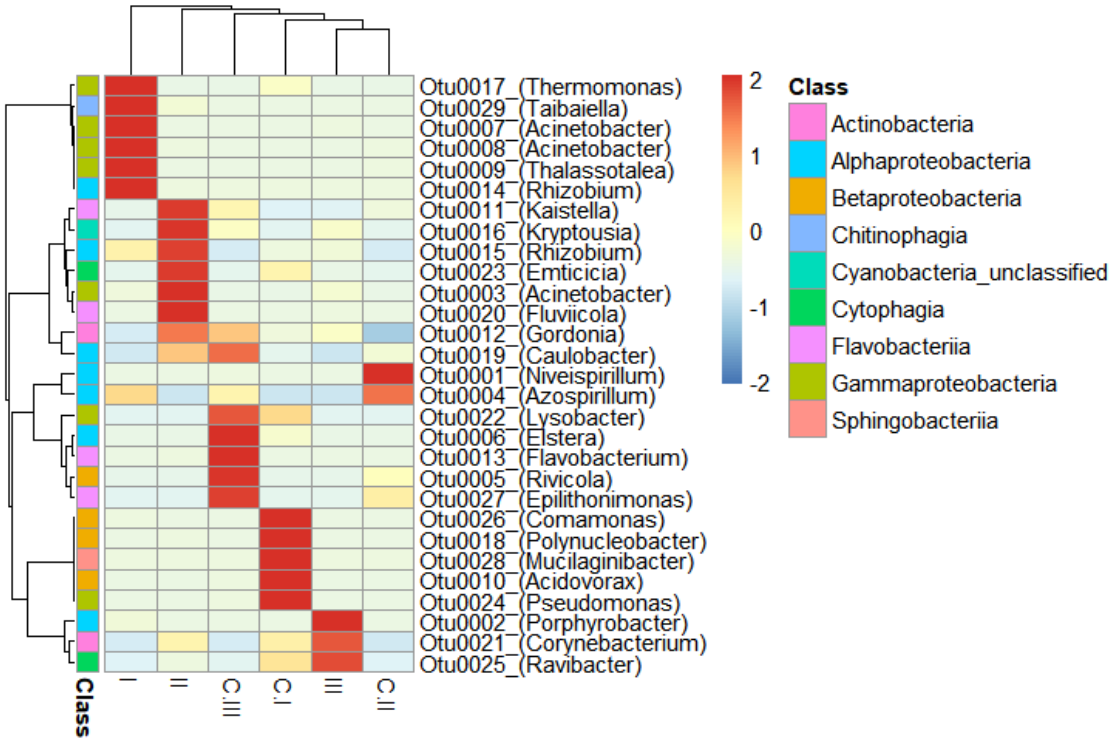

b)

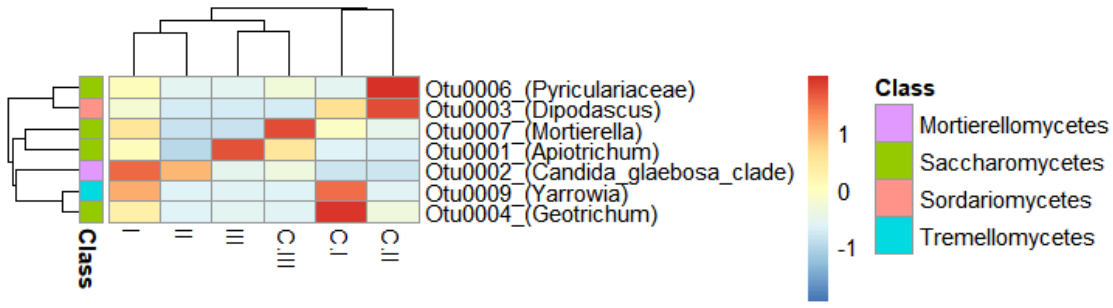

Table SI.1. Characterization of the waste fish oil used as a substrate (a) and composition of the stream used for dilution (b).

a) Waste fish oil: carbon source (2 mL/cycle)

Parameter		Value
pH		3.75 ± 0.20
Electrical conductivity	µS/cm	0.60 ± 0.10
Density	g/L	900 ± 10
$_t$COD	g/g	2.50 ± 0.11
Lipids	g/g	0.823 ± 0.089
TS	g/g	0.853 ± 0.018
VS	g/g	0.852 ± 0.019
Elemental analysis	%	N, C, H, S 0.00, 87.41, 14.11, 0.00
Fatty acids profile	wt %	Palmitic, stearic, oleic, linoleic, others 10.3 ± 0.4, 2.5 ± 1.0, 38.3 ± 1.6, 31.2 ± 1.5, 17.7 ± 4.2

b) Synthetic dilution water stream (2 L/cycle)

Compound		Value
NH_4Cl [(1)]	mg/L	600
$MgSO_4$	mg/L	140
KCl	mg/L	100
KH_2PO_4	mg/L	750 - 1000
$NaHCO_3$	mg/L	200 - 250
ATU	mg/L	2.5
NaCl	mg/L	10000
Trace element solution [(2)]	ml/L	2

ATU (allylthiourea), total chemical oxygen demand ($_t$COD), total solids (TS), volatile solids (VS).

[(1)] Addition during period I (coupled configuration). In periods II and III, no NH_4Cl was added in the dilution water. It was fed separately 20 mL of a concentrated solution containing 20 – 22 NH_4Cl g /L.

[(2)] Vishniac, W., Santer, M., 1957. The *thiobacilli*. Bacteriol. Rev. 21, 195–213.

Table SI 2. Characteristics of SBR-S operational periods and cycles monitored in the SBR-S and FBR-S.

		Period I (days 1 – 62)	**Period II (days 63 – 85)**	**Period III (Days 86 – 122)**
Selection strategy		Conventional ADF	DGL	DGL
C & N supply		Coupled. Simultaneous addition at the beginning of the cycle.	Uncoupled. C feeding at the beginning of the cycle and N supply at the end of the feast phase.	Uncoupled. C feeding at the beginning of the cycle and N supply at the end of the feast phase.
Nitrogen addition	mg TN/cycle	234	187	187
Buffer addition	g $NaHCO_3$/cycle	1	1	0.8
SBR-S cycle	Day of operation	22	85	106
FBR-S assay	Day of operation	29	85	106

Aerobic dynamic feeding (ADF), double growth limitation strategy (DGL), fed-batch reactor operated under saline conditions (FBR-S), sequential batch reactor operated under saline conditions (SBR-S), total nitrogen (TN).

Table SI 3. Relative abundance in percentage (n=2) ± SD of the main bacterial class (abundance > 0.05%) in biomass samples from FBR-S and FBR-C in periods I – III, identified by high-throughput Illumina sequencing.

		FBR-S						FBR-C					
		I		II		III		I		II		III	
Actinobacteria	*Acidimicrobiia*	0.01 ± 0.00	C	0.87 ± 0.00	A	0.14 ± 0.05	B	2.32 ± 0.58	A	0.01 ± 0.01	C	0.29 ± 0.00	B
	Actinobacteria	1.24 ± 0.01	B	8.62 ± 0.21	A	6.64 ± 1.80	A	5.91 ± 0.45	B	0.40 ± 0.10	C	7.94 ± 0.04	A
	Thermoleophilia	0.00 ± 0.00	C	0.25 ± 0.01	A	0.09 ± 0.03	B	0.21 ± 0.02	A	0.02 ± 0.00	C	0.07 ± 0.00	B
Armatimonadetes	*Fimbriimonadia*	0.00 ± 0.00	A	0.00 ± 0.00	A	0.00 ± 0.00	A	1.39 ± 0.33	A	0.01 ± 0.00	C	0.27 ± 0.02	B
Bacteroidetes	*Bacteroidia*	0.03 ± 0.01	B	0.58 ± 0.01	A	0.00 ± 0.00	C	0.07 ± 0.01	B	0.30 ± 0.00	A	0.03 ± 0.02	C
	Chitinophagia	2.77 ± 0.10	A	0.77 ± 0.04	B	0.02 ± 0.01	C	1.25 ± 0.30	B	0.69 ± 0.11	C	2.19 ± 0.00	A
	Cytophagia	0.01 ± 0.00	C	4.26 ± 0.05	A	2.66 ± 1.02	B	3.31 ± 0.54	A	0.07 ± 0.01	C	0.28 ± 0.02	B
	Flavobacteriia	2.38 ± 0.14	B	15.64 ± 0.37	A	0.41 ± 0.12	C	0.64 ± 0.09	C	2.02 ± 0.25	B	18.41 ± 0.06	A
	Sphingobacteriia	0.04 ± 0.01	B	0.28 ± 0.03	A	0.01 ± 0.00	C	3.31 ± 2.06	A	0.57 ± 0.00	B	2.41 ± 0.06	A
Chlamydiae	*Chlamydiia*	0.00 ± 0.00	C	0.09 ± 0.00	A	0.02 ± 0.01	B	0.25 ± 0.19	A	0.03 ± 0.00	A	0.23 ± 0.02	A
Cyanobacteria	*Cyanobacteria unclassified*	0.02 ± 0.01	C	6.48 ± 0.24	A	1.95 ± 0.63	B	0.05 ± 0.03	C	0.10 ± 0.02	B	2.27 ± 0.07	A
Firmicutes	*Bacilli*	0.00 ± 0.00	A	0.00 ± 0.00	A	0.00 ± 0.00	A	1.60 ± 0.55	A	0.01 ± 0.00	C	0.02 ± 0.00	B
	Clostridia	0.01 ± 0.00	C	2.37 ± 0.18	A	0.37 ± 0.15	B	1.58 ± 0.00	A	0.03 ± 0.00	C	0.20 ± 0.01	B
Gemmatimonadetes	*Gemmatimonadetes*	0.00 ± 0.00	A	0.00 ± 0.00	A	0.00 ± 0.00	A	0.10 ± 0.02	A	0.00 ± 0.00	B	0.00 ± 0.00	B
Proteobacteria	*Alphaproteobacteria*	29.11 ± 0.17	B	23.61 ± 0.57	C	79.30 ± 5.06	A	11.56 ± 1.85	C	88.85 ± 1.05	A	31.40 ± 0.07	B
	Betaproteobacteria	0.07 ± 0.00	B	0.15 ± 0.01	A	0.18 ± 0.05	A	33.49 ± 1.75	A	6.28 ± 0.48	C	28.48 ± 0.51	B
	Deltaproteobacteria	0.00 ± 0.00	C	0.25 ± 0.02	A	0.02 ± 0.01	B	1.76 ± 0.38	A	0.12 ± 0.02	C	0.21 ± 0.01	B
	Epsilonproteobacteria	0.00 ± 0.00	C	0.21 ± 0.02	A	0.08 ± 0.04	B	1.59 ± 0.93	A	0.00 ± 0.00	C	0.32 ± 0.04	B
	Gammaproteobacteria	64.28 ± 0.11	A	34.94 ± 1.80	B	8.07 ± 1.13	C	21.42 ± 5.82	A	0.30 ± 0.02	C	3.75 ± 0.12	B
	Oligoflexia	0.00 ± 0.00	B	0.07 ± 0.00	A	0.00 ± 0.00	B	1.93 ± 0.46	A	0.05 ± 0.02	C	0.31 ± 0.00	B

Capital letters (A, B, C) indicate statistical differences among the operational periods for a given reactor, according to Kruskal-Wallis (Conover-Iman *posthoc* test, $p < 0.05$).

Table SI 3 (Continuation)

		FBR-S						FBR-C					
		I		II		III		I		II		III	
Verrucomicrobia	*Opitutae*	0.02 ± 0.00	B	0.16 ± 0.01	A	0.00 ± 0.00	C	1.08 ± 0.60	A	0.02 ± 0.00	C	0.43 ± 0.00	B
	Spartobacteria	0.00 ± 0.00	A	0.00 ± 0.00	A	0.00 ± 0.00	A	0.78 ± 0.23	A	0.00 ± 0.00	B	0.00 ± 0.00	B
	Verrucomicrobiae	0.00 ± 0.00	B	0.02 ± 0.01	A	0.00 ± 0.00	B	2.99 ± 0.42	A	0.00 ± 0.00	C	0.30 ± 0.01	B
Bacterial Minority classes		0.00 ± 0.00	C	0.36 ± 0.06	A	0.04 ± 0.01	B	1.43 ± 0.53	A	0.11 ± 0.03	C	0.19 ± 0.02	B

Capital letters (A, B, C) indicate statistical differences among the operational periods for a given reactor, according to Kruskal-Wallis (Conover-Iman *posthoc* test, $p < 0.05$).

Table SI 4. Relative abundance in percentage (n=2) ± SD of the main fungal classes (abundance>0.05%) in activated sludge samples from FBR-S and FBR-C in periods I – III, identified by high-throughput Illumina sequencing. Capital letters indicate statistical differences among the operational periods for a given reactor, according to Kruskal-Wallis (Conover-Iman *posthoc* test, $p < 0.05$).

		FBR-S						**FBR-C**					
		I		**II**		**III**		**I**		**II**		**III**	
Ascomicota	*Dothideomycetes*	0.02 ± 0.02	A	0.01 ± 0.01	A	0.16 ± 0.22	A	0.56 ± 0.77	A	n.d.	B	0.14 ± 0.17	A
	Saccharomycetes	50.10 ± 0.28	B	83.42 ± 2.08	A	14.74 ± 0.66	C	67.83 ± 2.95	A	56.11 ± 1.03	B	21.66 ± 1.41	C
	Sordariomycetes	4.06 ± 3.66	A	0.03 ± 0.02	B	n.d.	C	0.27 ± 0.38	C	16.57 ± 3.08	A	1.94 ± 1.05	B
Basidiomycota	*Agaricomycetes*	n.d.	A	n.d.	A	n.d.	A	0.65 ± 0.46	A	0.70 ± 0.07	A	0.02 ± 0.00	A
	Cystobasidiomycetes	1.15 ± 1.63	A	0.00 ± 0.01	A	n.d.	A	n.d.	A	n.d.	A	n.d.	A
	Microbotryomycetes	1.35 ± 1.54	A	0.01 ± 0.01	B	n.d.	B	n.d.	B	n.d.	B	1.67 ± 0.30	A
	Tremellomycetes	43.32 ± 3.83	B	16.41 ± 2.06	C	85.10 ± 0.44	A	24.97 ± 1.52	B	23.89 ± 2.15	B	55.14 ± 3.93	A
Mucoromycota	*Mortierellomycetes*	n.d.	B	0.04 ± 0.01	A	n.d.	B	5.69 ± 2.89	B	2.46 ± 0.12	C	19.41 ± 4.38	A
Fungal Minority classes		0.03 ± 0.03	B	0.25 ± 0.06	A	0.03 ± 0.03	B	n.d.	B	0.07 ± 0.02	A	n.d.	B

Capital letters (A, B, C) indicate statistical differences among the operational periods for a given reactor, according to Kruskal-Wallis (Conover-Iman *posthoc* test, $p < 0.05$).

Table SI 5. Relative abundance in percentage (n = 2) ± SD of the main bacterial OTUs in biomass samples from FBR-S and FBR-C in periods I – III, identified by high-throughput Illumina sequencing.

	FBR-S									FBR-C								
	I			II			III			I			II			III		
OtuB0001(*Niveispirillum*)	n.d.	C	a	0.05 ± 0.01	A	a	0.03 ± 0.00	B	a	0.04 ± 0.02	C	a	72.73 ± 1.36	A	a	0.17 ± 0.02	B	a
OtuB0002(*Porphyrobacter*)	4.06 ± 0.10	B	a	0.40 ± 0.02	C	a	74.13 ± 5.57	A	a	0.02 ± 0.01	A	a	0.02 ± 0.00	A	a	n.d.	B	a
OtuB0003(*Acinetobacter*)	2.21 ± 0.12	C	a	34.62 ± 1.84	A	a	4.19 ± 0.59	B	a	0.42 ± 0.12	A	b	0.04 ± 0.00	C	b	0.22 ± 0.01	B	b
OtuB0004(*Azospirillum*)	10.20 ± 0.24	A	a	0.02 ± 0.01	B	a	0.01 ± 0.01	B	a	0.01 ± 0.00	C	a	14.83 ± 0.25	A	a	6.71 ± 0.02	B	a
OtuB0005(*Rivicola*)	n.d.	A	b	n.d.	A	b	n.d.	A	b	n.d.	C	a	5.07 ± 0.20	B	a	26.21 ± 0.63	A	a
OtuB0006(*Elstera*)	n.d.	A	b	n.d.	A	b	n.d.	A	b	1.40 ± 0.96	B	a	0.01 ± 0.00	C	a	21.54 ± 0.03	A	a
OtuB0007(*Acinetobacter*)	18.94 ± 0.17	A	a	0.02 ± 0.00	C	a	0.35 ± 0.11	B	a	0.06 ± 0.04	A	a	0.04 ± 0.01	A	a	n.d.	B	a
OtuB0008(*Acinetobacter*)	18.05 ± 0.13	A	a	0.01 ± 0.00	B	a	n.d.	B	a	n.d.	B	a	0.02 ± 0.00	A	a	n.d.	B	a
OtuB0009(*Thalassotalea*)	16.43 ± 0.33	A	a	0.01 ± 0.00	B	a	n.d.	B	a	n.d.	B	a	0.01 ± 0.00	A	a	n.d.	B	a
OtuB0010(*Acidovorax*)	n.d.	A	a	0.01 ± 0.00	A	a	n.d.	A	a	18.73 ± 9.11	A	a	0.01 ± 0.00	C	a	0.09 ± 0.00	B	a
OtuB0011(*Kaistella*)	0.61 ± 0.08	B	a	9.62 ± 0.23	A	a	0.36 ± 0.11	C	a	0.01 ± 0.00	C	a	1.31 ± 0.04	B	a	3.15 ± 0.02	A	a
OtuB0012(*Gordonia*)	0.94 ± 0.02	C	a	4.58 ± 0.06	A	a	2.75 ± 0.75	B	a	1.52 ± 0.10	B	a	0.26 ± 0.05	C	a	3.54 ± 0.02	A	a
OtuB0013(*Flavobacterium*)	n.d.	B	a	0.11 ± 0.00	A	a	n.d.	B	a	n.d.	B	a	n.d.	B	a	12.57 ± 0.11	A	a
OtuB0014(*Rhizobium*)	10.44 ± 0.14	A	a	n.d.	B	a	n.d.	B	a	n.d.	A	a	n.d.	A	a	n.d.	A	a
OtuB0015(*Rhizobium*)	2.36 ± 0.06	B	a	6.50 ± 0.17	A	a	1.12 ± 0.08	C	a	0.63 ± 0.27	A	b	n.d.	C	b	0.01 ± 0.00	B	b
OtuB0016(*Kryptousia*)	0.01 ± 0.01	C	a	6.41 ± 0.23	A	a	1.56 ± 0.46	B	a	0.01 ± 0.01	C	b	0.10 ± 0.01	B	b	1.28 ± 0.05	A	b
OtuB0017(*Thermomonas*)	6.53 ± 0.04	A	a	0.02 ± 0.00	B	a	n.d.	C	a	2.39 ± 1.42	A	a	0.02 ± 0.00	B	a	n.d.	C	a
OtuB0018(*Polynucleobacter*)	n.d.	A	a	n.d.	A	a	n.d.	A	a	6.93 ± 4.26	A	a	n.d.	B	a	n.d.	B	a
OtuB0019(*Caulobacter*)	0.11 ± 0.03	B	a	1.91 ± 0.17	A	a	0.07 ± 0.02	B	a	0.26 ± 0.09	C	a	0.56 ± 0.03	B	a	2.36 ± 0.09	A	a
OtuB0020(*Fluviicola*)	n.d.	C	a	4.92 ± 0.11	A	a	0.03 ± 0.01	B	a	n.d.	A	a	n.d.	A	a	n.d.	A	a
OtuB0021(*Corynebacterium*)	0.05 ± 0.01	C	a	0.88 ± 0.04	B	a	2.88 ± 0.80	A	a	0.76 ± 0.16	A	b	n.d.	C	b	0.03 ± 0.01	B	b

Capital letters (A, B, C) indicate statistical differences among the operational periods for a given reactor according to the Kruskal-Wallis (Conover-Iman *posthoc* test, $p < 0.05$).
Lowercase letters (a, b, c) indicate statistical differences between reactors, according to the Mann-Whitney ($p < 0.05$).

Table SI 5 (continuation)

	FBR-C																	
	I			**II**			**III**			**I**			**II**			**III**		
OtuB0022(Lysobacter)	n.d.	A	b	n.d.	A	b	n.d.	A	b	1.75 ± 0.08	B	a	n.d.	C	a	2.87 ± 0.08	A	a
OtuB0023(*Emticicia*)	n.d.	C	a	3.58 ± 0.06	A	a	0.26 ± 0.12	B	a	0.62 ± 0.46	A	a	n.d.	B	a	n.d.	B	a
OtuB0024(*Pseudomonas*)	n.d.	A	a	n.d.	A	a	n.d.	A	a	4.74 ± 2.38	A	a	n.d.	C	a	0.01 ± 0.00	B	a
OtuB0025(*Ravibacter*)	n.d.	C	a	0.16 ± 0.00	B	a	2.20 ± 0.80	A	a	1.45 ± 0.77	A	a	n.d.	C	a	0.04 ± 0.00	B	a
OtuB0026(*Comamonas*)	0.01 ± 0.00	A	a	n.d.	A	a	n.d.	A	a	2.88 ± 1.57	A	a	n.d.	B	a	n.d.	B	a
OtuB0027(*Epilithonimonas*)	n.d.	A	b	n.d.	A	b	0.01 ± 0.00	A	b	0.04 ± 0.00	C	a	0.69 ± 0.29	B	a	2.63 ± 0.03	A	a
OtuB0028(*Mucilaginibacter*)	n.d.	A	a	n.d.	A	a	n.d.	A	a	2.67 ± 1.70	A	a	n.d.	B	a	n.d.	B	a
OtuB0029(*Taibaiella*)	2.76 ± 0.10	A	a	0.22 ± 0.00	B	a	0.01 ± 0.01	C	a	n.d.	A	b	n.d.	A	b	n.d.	A	b

Capital letters (A, B, C) indicate statistical differences among the operational periods for a given reactor according to the Kruskal-Wallis (Conover-Iman *posthoc* test, $p < 0.05$).
Lowercase letters (a, b, c) indicate statistical differences between reactors, according to the Mann-Whitney ($p < 0.05$).

Table SI 6. Relative abundance in percentage (n = 2) ± SD of the main fungal OTUs in activated sludge samples from FBR-S and FBR-C, identified by high-throughput Illumina sequencing.

	FBR-S									FBR-C								
	I			II			III			I			II			III		
OtuF0001(*Apiotrichum*)	43.29 ± 2.71	B	a	16.39 ± 1.46	C	a	85.03 ± 0.30	A	a	24.93 ± 1.07	B	a	23.84 ± 1.51	B	a	54.48 ± 2.97	A	a
OtuF0002(*Candida glaebosa clade*)	33.06 ± 1.29	B	a	82.92 ± 1.32	A	a	13.07 ± 0.02	C	a	1.01 ± 0.06	B	a	1.22 ± 0.21	B	a	20.89 ± 0.95	A	a
OtuF0003(*Dipodascus*)	0.83 ± 0.83	A	b	0.02 ± 0.00	A	b	0.01 ± 0.00	A	b	27.37 ±10.04	B	b	50.13 ± 0.21	A	b	0.00 ± 0.00	C	b
OtuF0004(*Geotrichum*)	13.27 ± 0.88	A	a	0.03 ± 0.01	C	a	1.27 ± 0.73	B	a	35.29 ± 7.50	A	a	4.23 ± 0.15	B	a	0.55 ± 0.12	C	a
OtuF0006(*Pyriculariaceae*)	4.06 ± 2.59	A	a	0.02 ± 0.01	B	a	0.00 ± 0.00	C	a	0.00 ± 0.00	C	a	16.44 ± 2.05	A	a	1.94 ± 0.74	B	a
OtuF0007(*Mortierella*)	0.00 ± 0.00	B	a	0.04 ± 0.01	A	a	0.00 ± 0.00	B	a	5.69 ± 2.05	B	b	2.46 ± 0.08	C	b	19.41 ± 3.10	A	b
OtuF0009(Yarrowia)	2.50 ± 0.36	A	a	0.01 ± 0.00	B	a	0.10 ± 0.10	B	a	3.22 ± 0.27	A	a	0.08 ± 0.08	B	a	0.00 ± 0.00	B	a

Capital letters (A, B, C) indicate statistical differences among the operational periods for a given reactor according to the Kruskal-Wallis (Conover-Iman *posthoc* test, $p < 0.05$).
Lowercase letters (a, b, c) indicate statistical differences between reactors, according to the Mann-Whitney ($p < 0.05$).

Highlights

- TAG and PHA were recovered from industrial waste fish oil under saline conditions.
- Uncoupled C & N feeding was advantageous for PHA producers despite salinity.
- Salinity drove the medium pH to neutrality so $NaHCO_3$ buffer might be avoided.
- PHA-accumulators were more sensitive to high salinity than TAG-accumulators.
- Osmotic stress specifically modulated the structure of the microbial community.

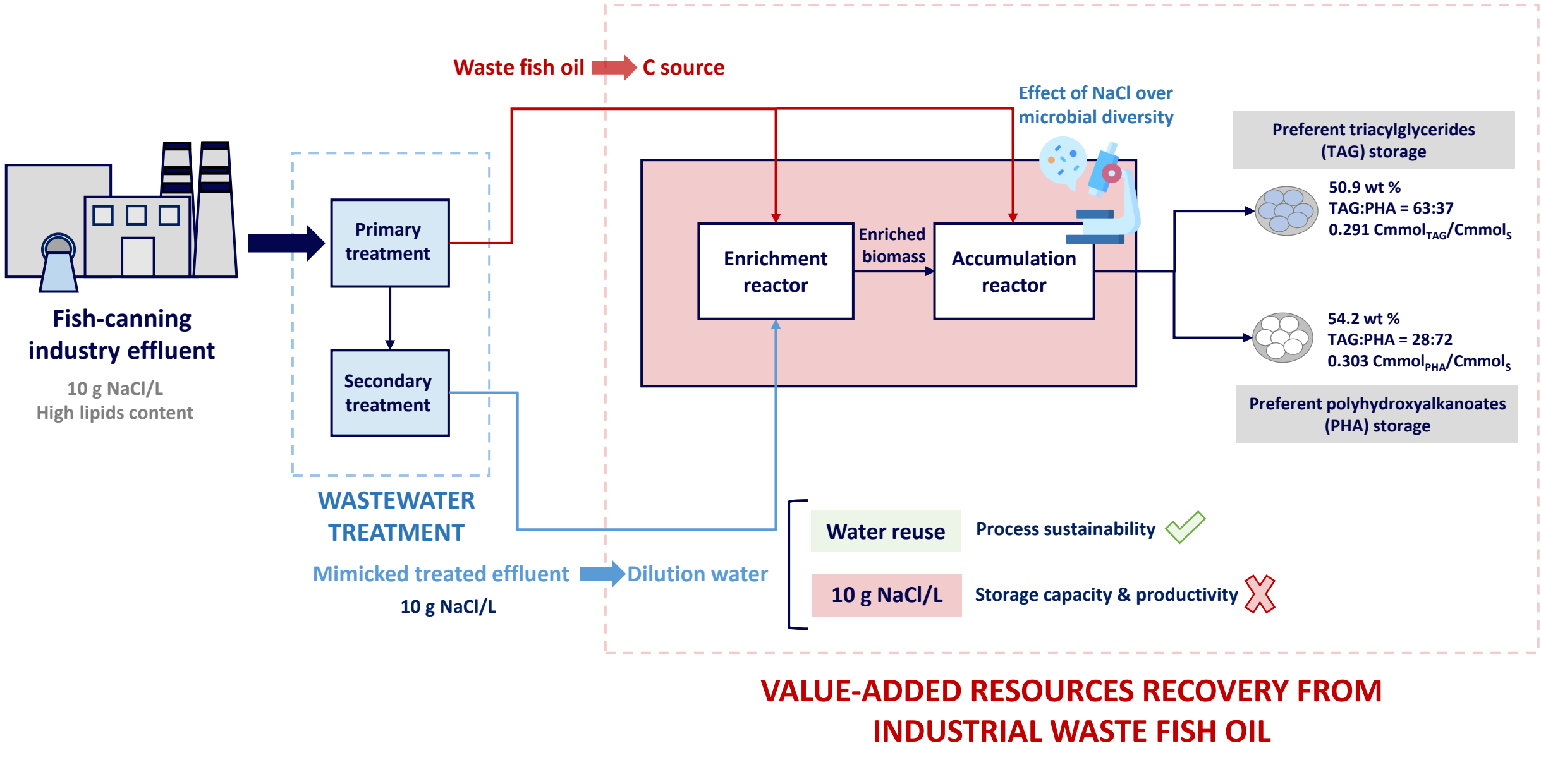

VALUE-ADDED RESOURCES RECOVERY FROM INDUSTRIAL WASTE FISH OIL